X-640-67-29

TEMPORAL VARIATIONS OF MESOSPHERIC OXYGEN AND OZONE DURING AURORAL EVENTS

BY

KAICHI MAEDA

A. C. AIKIN

JANUARY 1967

GODDARD SPACE FLIGHT CENTER

GREENBELT, MARYLAND

TEMPORAL VARIATIONS OF MESOSPHERIC OXYGEN AND OZONE DURING AURORAL EVENTS

by

Kaichi Maeda and A. C. Aikin

Goddard Space Flight Center
Greenbelt, Maryland

TEMPORAL VARIATIONS OF MESOSPHERIC OXYGEN AND OZONE DURING AURORAL EVENTS

by

Kaichi Maeda and A. C. Aikin

ABSTRACT

Temporal solutions are given of the photo-chemical equations describing the distribution of ozone and atomic oxygen in an oxygen atmosphere for the equatorial and polar regions. Similar calculations are applied to auroral events, and indicate a strong dependence of mesospheric atomic oxygen on the intensity and energy spectrum of auroral electrons, which dissociate molecular oxygen. It is shown that there can be no significant atmospheric ozone and atomic oxygen modifications due to soft spectrum electron events which appear to characterize most bright auroras. On the other hand, the hard spectrum auroral electrons which appear in most weak, quiet auroras should cause significant increases in the atomic oxygen and ozone concentration below 80 km, provided their flux is more than 10^6 per cm^2 sec.

CONTENTS

TEMPORAL VARIATIONS OF MESOSPHERIC OXYGEN AND OZONE DURING AURORAL EVENTS

1. INTRODUCTION

The dissociation of molecular oxygen by ultraviolet radiation and charged particles, and the subsequent reaction of atomic oxygen with molecular oxygen to form ozone in the earth's atmosphere was first considered by Chapman (1930). Since then, the chemical equations describing the distribution of ozone and atomic oxygen in the mesosphere have been considered by numerous investigators including Bates and Nicolet (1950), Dütsch (1961), Barth (1961), Wallace (1962), Hesstvedt (1963), Leovy (1964) and Hunt (1964; 1965; 1966 a,b). None of these treatments has considered the effect of auroral electrons as a source of molecular dissociation in addition to solar radiation.

Maeda (1963) has made use of laboratory experiments on the dissociation of oxygen by electron impact (Glockler and Wilson, 1932; Massey and Burhop, 1956) to estimate the dissociation rate of molecular oxygen due to auroral electrons and protons. However, more accurate estimates of the electron impact dissociation cross section as a function of electron energy have recently been reported (Lassettre, Silverman, and Krasnow, 1964; Silverman and Lassettre, 1964; and Bauer and Bartky, 1965). In this paper the new data on 0_2-dissociation by electron impact will be employed to reevaluate the rate coefficient for dissociation by auroral electrons. More rigorous computations are made of electron diffusion in the upper atmosphere in which energy loss, coulomb scattering

and the effects of straggling are simultaneously taken into account (Maeda, 1965a, b).

The resulting rate coefficients are then applied to the calculation of the temporal variation of ozone and atomic oxygen in the mesosphere during auroral events. This is accomplished by solving the time dependent photo-chemical equations for a pure oxygen atmosphere in the 50 to 120 km region. The modification of the ionosphere due to the change in concentration of 0 and 0_3 during charged particle bombardment will be discussed.

The effect of including diffusion is discussed in Appendix C. Reactions involving hydrogen and exicted states of atomic oxygen, and the dissociation due to secondary and tertiary electrons resulting from PCA protons will be discussed in a separate report.

2. DISSOCIATION OF OXYGEN MOLECULES BY ELECTRON IMPACT

Figures 1 and 2 illustrate the potential energy curves for molecular oxygen and the energy level diagram of atomic oxygen, respectively. Excitation of the molecule to repulsive energy levels will lead eventually to the dissociation of the molecule, for which the minimum energy is 5.08 eV. Photon absorption cross sections in the Schumann Runge continuum have been measured accurately by Watanabe et al. (1953) as well as Ditchburn and Young (1962). Recently cross sections have been determined accurately for dissociation of oxygen by electron impact.

Dissociative reactions of oxygen by electron impact can be categorized as follows:

$$0_2 + e \rightarrow 0 + 0^- \qquad (2.1)$$

$$\rightarrow O + O^* + e \tag{2.2}$$

$$\left.\begin{array}{l} O + O^+ + 2e \\ \rightarrow O^- + O^+ + e \\ O^+ + O^+ + 3e \end{array}\right\} \tag{2.3}$$

Reaction (2.1) - This is the resonance capture of an electron or the so-called resonance dissociative attachment having a maximum at 6.5 eV (Massey, 1950). The total cross section for dissociative attachment based on recent measurements by Rapp and Briglia (1964) and Rapp, Sharp and Briglia (1964) is given in Figure 3. The maximum cross section for this reaction occurring at 6.5 eV is 1.5×10^{-18} cm^2.

Reaction (2.2) - The dissociation of O_2 into two neutral atoms is of most interest to us. The inelastic scattering of electrons of incident energy 4.5 to 12.5 eV has been studied by Schulz and Dowell (1962). Their results are reproduced in Figure 4. The peak in the cross section of 6.5 eV undoubtedly corresponds to (2.1).

The major peak occurs at 8.44 eV and is due to dissociation from the excited state ($B\,^3\Sigma_u^-$). Dissociation from this level will lead to one atom in the ^3P ground state and one metastable ^1D atom as can be seen from Figures 1 and 2. The peak at 9.0 eV results from dissociation from the $^1\Delta_u$ state leading to two ^1D atoms. Other peaks up to the first ionization potential at 12.04, McGowan et al. (1964), are also discernable. Schulz has estimated the cross section and finds a value of about 1.9×10^{-18} cm^2 at the 8.44 eV peak. The cross section has also been estimated chemically (Gockler and Wilson, 1932; Massey and Burhop, 1956). From an analysis of d.c. discharges in oxygen gas, Thompson

(1959) estimates that the cross section for dissociation of oxygen by electrons of energy greater than 14 eV is at least an order of magnitude greater than that for excitation to the $^1\Delta_g$ state.

The most recent experimental work on the cross section for dissociation of oxygen by electrons whose energy is greater than 20 eV has been accomplished by Lassettre (1959) who found that the cross section for dissociation by electron of 500 eV incident energy was 10 percent of the total cross section. Lassettre et al (1964) have shown that the cross section for energy loss at 8.44 eV by 500 eV electron is 4×10^{-16} cm^2. Most of the dissociations result from this reaction, which is a source of $O(^1D)$.

The oscillator strength derived from the experimental data at 500 eV together with the Born approximation have been used by Silverman and Lassettre (1964) to derive the dissociation cross section as a function of incident electron energy. This cross section as a function of energy is reproduced in Figure 3. Also shown is the result of a calculation by Bauer and Barkly (1965) based on the classical theory of Gryzinski (1959) and employing the potential energy diagram given by Gilmore (1964), Figure 1. Silverman and Lassettre (1964) regard their calculations as a lower bound on the dissociation cross section since only one transition has been included. It should be noted that O_2 dissociation by electron impact is far larger than that of photo-dissociation in the same energy range. Also given in the figure are cross sections employed by Maeda (1962, 1963).

No information is available on the dissociation of ozone by electron impact. It will be assumed for the purposes of calculation that the cross section is at least as large as that given for O_2.

Reaction (2.3) – This is the dissociative ionization of oxygen. Frost and McDowell (1958) have studied reactions of this type and found that as the colliding electron energy increases not only 0^+ but also 0^-, 0 and 0^{++} will be produced.

The cross section σ_i, for 0_2 ionization as measured by laboratory experiments is also shown in Figure 3, (Tate and Smith, 1932). The dashed curve at the low energy end of this data is an extrapolation assuming that the ionization cross section vanishes below the 0_2 ionization potential.

3. AURORAL DISSOCIATION OF ATMOSPHERIC OXYGEN MOLECULES

3.1 Dissociation by Monoenergetic Electrons

The energy of most auroral electrons is between 5 and 50 kev, except for occasional hard-spectrum auroral electron events. (McIlwain, 1960; Chamberlain, 1961, p. 269; Hultquist, 1964; Mann et al., 1963). Since the results of calculations made for monoenergetic electrons can be applied to more general cases of different energy spectra, computations are first performed for several cases of monoenergetic electrons.

Any charged particle impinging into the earth's atmosphere follows a spiral orbit along a geomagnetic line of force. It can be shown, however, that if the magnetic field is uniform and vertical, the effect of spiral motion on the diffusion of charged particles in the atmosphere can be disregarded except for the estimation of the horizontal spread in the atmosphere (Maeda and Singer, 1961; Maeda, 1962; 1963). These charged particles entering into denser atmosphere undergo simultaneously multiple Coulomb scattering and energy-loss by collisions with air molecules in the upper atmosphere.

Because of its smallness in mass, angular spreads of scattered electrons at each collision are very large as compared with those of protons or heavier

particles of the same velocity. Furthermore, their energy losses at each collision are not uniform but fluctuate wildly, causing the so-called straggling effect in their residual range, i.e., the penetration depth. Due to the statistical nature of these scattering and of energy losses, diffusion of electrons into the atmosphere has not been calculated rigorously until recently (Spencer, 1959; Rees, 1963; Maeda, 1965 a, b).

The rate of dissociation of atmospheric oxygen, $J_d(z, E_0)$, by monoenergetic incident electrons, E_0, at the altitude z, can be given by

$$J_{de}(z, E_0) = \int_0^{E_0} N(z) \left[\int_{E_c}^{E_0} \sigma_d(w)\, j_e(W, E, z)\, dW \right] i(E, E_0 z)\, dE \cdot dz \qquad (3.1)$$

where

$N(z)$ is the number density of molecular oxygen at the altitude z, (cm^{-3}),

$\sigma_d(W)$ is the differential cross-section of O_2-dissociation by electrons with energy W (cm^2, W in kev) and shown in Fig. 3 by σ_{SL}, σ_M, and σ_{BB}.

$j_e(W, E, z)$ is the number of secondary electrons of energy between W and $W + dW$, produced by electrons of energy E per unit thickness of air at the altitude z, $(cm^{-1}$, z in km).

$i(E, E_0, z)$ is the number of electrons with energies between E and $E + dE$ at the height z, corresponding to the incident energy E_0, i.e., the differential energy spectrum of electrons in energy E and $E + dE$ at the altitude z, in the atmosphere normalized to the incident total flux of monoenergetic electrons of E_0, $(cm^{-2}\ sec^{-1})$.

E_c (5 eV) is the threshold energy for O_2-dissociation.

The terms inside the square bracket of the integrand (3.1) can be written as:

$$\int_{E_c}^{E} \sigma_d(w)\, j(W, E, z)\, dW \simeq \sigma_t \cdot j_t(E) \cdot \rho(z) \tag{3.2}$$

where

$$\sigma_t = \frac{1}{W_e} \int_{E_c}^{\infty} \sigma_d(W)\, dW \tag{3.3}$$

W_e ($\simeq 20$ eV) is the effective energy for 0_2-dissociation.

$\rho(z)$ is the density of air (in g cm^{-3}) at the altitude z (in km),

$j_t(E)$ is the number of secondary electrons per primary electron with energy E (kev) per unit thickness of air (g cm^{-2}). This is shown in Fig. 5 as a function of E (kev).

In Fig. 5, the curve below 1 kev is derived from the experimental data for gases 0_2 and N_2 (Tate and Smith, 1932); and the residual portion, particularly above 10 kev, is computed by the following formula:

$$j_t(E) = \frac{k(E)}{V_0} \tag{3.4}$$

where $V_0 \simeq 32$ eV (Rossi, 1952, p. 47), and $k(E)$ is the rate of ionization loss of electrons with energy E in air given by the Bethe formula (Wu, 1960, p. 17).

The differential spectrum of elections, $i(E, E_0, z)$, at the altitude z in Eq. (3.1) is computed from $i(E, E_0, x)$, the spectrum at the atmospheric depth x, by making use of $x-z$ relation for the CIRA-atmosphere (1965).

If the ionization loss, coulomb scattering and the effect of straggling are to be taken into consideration simultaneously, then $i(E, E_0, x)$ can be calculated only by the Monte Carlo method.

In the present calculations, $i(E, E_0, x)$ is expressed by an analytic formula as shown in Appendix A. A comparison of this expression with the result obtained by Monte Carlo calculation is shown in Fig. 6 for the case of vertically incident mono-energetic electrons, $E_0 = 20$ kev. The total intensity $I(E_0, \xi)$ is also expressed by an empirical formula, (Appendix A), which is shown in Fig. 7 with results obtained by Monte Carlo calculation (for $E_0 = 20$ kev). In the same figure, Monte Carlo result of the total energy flux variation with penetration depth in air $E(\xi)/E_0$ is also plotted against $\xi = x/r_0$.

Final results of $J_{de}(z)$ cm^{-3} sec^{-1}, are shown in Fig. 8, as a function of altitude, z (in Km) for vertically incident monoenergetic electrons with initial energy range $5\ keV \leq E_0 \leq 1$ Mev.

By using the approximation (3.2), the right hand side of Eq. (3.1) is written as:

$$J_{de}(z, E_0) = \sigma_t \cdot N(z)\rho(z) \int_{E_c}^{E} j_t(E) \cdot i(E, E_0, z)\, dE\, dz \qquad (3.5)$$

As can be seen from this expression $J_{de}(z)$ is proportional to σ_t, the total cross-section of O_2-dissociation by electron impact. The scale of the abscissa $J_{de}(z)$ in Fig. 8 should be read, therefore, by multiplying a factor α, for different cases of reactions which are indicated by Eqs. (2.1), (2.2) and (2.3). The factor, α, and the effective energy W_e (in eV) for these reactions and cross sections are shown in Table 1. From this table one can see that the application of the Lassettre cross section increases the dissociation rate by a factor of 10 above that employed by Maeda (1963). The Lassettre value of cross section will be applied in all subsequent calculations of the dissociation effects of auroral electrons.

Table 1

Multiplication Factor, α, for $J_{de}(z)$ shown in Figure 6, Corresponding to Cross Sections and the Effective Energies $\bar{W}_e$

Reactions	Cross Section (Fig. 3)	α	$\bar{W}_e$ (eV)
(2.1)	σ_M	0.1	10
	σ_{SL}	1.0	80
	σ_{BB}	0.5	80
(2.2)	σ_i	2.0	150
(2.3)	σ^-	$<10^{-3}$	6

3.2 DISSOCIATION BY AURORAL ELECTRONS WITH EXPONENTIAL SPECTRA

It has been reported that the energy distribution of the primary auroral electrons, $i(E_0)$, is consistent with the following form of exponential spectrum rather than the single power-of-energy formula; a monoenergetic distribution, $\delta(E - E_0)$, is a fairly good approximation in most cases (McIlwain, 1960; Brown, 1964):

$$i(E_0) = i_0 \exp\left(-\frac{E_0}{E_a}\right) \tag{3.6}$$

where E_a is a constant (in keV).

The effect of the energy spectrum on the rate of dissociation can be calculated by making use of previous results for monoenergetic electrons as follows:

$$J_D(z) = \frac{\int_0^\infty J_{de}(z, E_0) \exp\left(-\frac{E_0}{E_a}\right) dE_0}{\int_0^\infty \exp\left(-\frac{E_0}{E_a}\right) dE_0} \simeq \frac{1}{E_a} \sum_{i=1}^{\infty} J_{de}(z, E_0^i) \exp\left(-\frac{E_0^i}{E_a}\right) \Delta E_0^i \tag{3.7}$$

where $J_{de}(z, E_0^i)$'s are given by Eq. (3.5) and shown in Fig. 8 as a function of the altitude z (km).

In Fig. 8, E_0^i is taken as a parameter for the range from 5 keV to 1 Mev and the altitude z is indicated in the abscissa. $J_D(z)$'s are computed for two cases, i.e., E_a = 5 keV and 100 keV. These are shown in Fig. 9 against the altitude z (in km).

4. PHOTOCHEMICAL REACTIONS FOR MESOSPHERIC OZONE AND ATOMIC OXYGEN

The amount of ozone above 50 km comprises less than one percent of the total ozone content in a vertical column of the atmosphere. However, a knowledge of its distribution and time variation is important in the study of the dynamics of the mesosphere, as well as airglow phenomena such as the OH band emission in the lower mesosphere (Bates and Nicolet, 1950; Wallace, 1962; Hunt, 1966b). Its role in the ionosphere as a possible attaching agent to form O_3^- has been discussed in terms of the twilight behavior of PCA absorption events, Reid (1964). The altitude distribution and temporal variation of atomic oxygen is also important from both the ionospheric and aeronomical standpoints. In this section the time dependent equations governing the distribution of ozone and atomic oxygen will be solved for an oxygen atmosphere. Prior to investigating the effect of auroral particles, calculations will be performed for both an equatorial and polar atmosphere under the influence of solar radiation. Since the equatorial distribution has been discussed by many investigators, the present calculation scheme can be compared with the results of others.

4.1 Equations and Constants

Principal reactions for ozone formation and destruction are shown in Table 2. The element M in the three-body collision is not necessarily oxygen, but any atom or molecule which balances the energies and momentum in the colliding reaction. The number density [M], is, therefore, given by the total number density of air. Although the importance of reactions involving hydrogen has been treated by Wallace (1962) and shown to be necessary to explain quantitatively the ozone distribution more recently by Hunt (1966b), only a pure oxygen atmosphere will be considered in the present investigation. Also the possible role of excited molecular states, Hunt (1965) Schiff and McGill (1964) will be discussed in a future report.

Table 2

Principal Reactions for Atmospheric Ozone

Formation and Destruction

(i) Ozone formation

$$O + O_2 + M \xrightarrow{k_{12}} O_3 + M$$

(ii) Ozone destruction

$$O + O_3 \xrightarrow{k_{13}} 2O_2$$

(iii) Atomic oxygen recombination

$$O + O + M \xrightarrow{k_{11}} O_2 + M$$

(iv) Dissociation of molecular oxygen

$$O_2 + h\nu \xrightarrow{\sigma_2} O + O \text{ for } \lambda < 2424\text{Å}$$

$$O_2 + e \xrightarrow{\alpha_2} O + O + e \text{ for } \longleftarrow E > 5 \text{ eV}$$

(v) Ozone dissociation

$$O_3 + h\nu \xrightarrow{\sigma_3} O + O_2 \text{ for } \lambda < 11800\text{Å}$$

$$O_3 + e \xrightarrow{\alpha_3} O + O_2 + e \text{ for } \longleftarrow E > 1 \text{ eV}$$

Corresponding to reactions shown in Table 2, time variations of odd-oxygen allotropes are given by the following two equations together with a similar equation for 0_2

$$\frac{d[0_3]}{dt} = k_{12}[0][0_2][M] - k_{13}[0][0_3] - J_3[0_3] \tag{4.1}$$

$$\frac{d[0]}{dt} = 2J_2[0_2] + J_3[0_3] - k_{12}[0][0_2][M] - k_{13}[0][0_3] - k_{11}2[0]^2[M] \tag{4.2}$$

where $[0]$, $[0_2]$, $[0_3]$ and $[M]$ are the number density of atomic oxygen, molecular oxygen, ozone and the total number density respectively. A summary of the values of the rate coefficients k_{11}, k_{12} and k_{13} employed in the present calculations is given in Table 3 together with the most recent laboratory determinations. As can be seen from the table, the reaction rate changes with atmospheric temperature, which is a function of altitude, latitude and season. Since the main purpose of the present calculation is to see the basic character of variation rather than to investigate many possible cases, the effect of atmospheric temperature will be ignored and will be discussed separately.

Table 3

Rate Coefficients

Reaction	Present Calculation	Rate	
k_{11} cm^6 sec^{-1}	3×10^{-33}	3×10^{-33}	(Reeves et al., 1960)
k_{12} cm^6 sec^{-1}	5×10^{-34}	8×10^{-35} exp (445/T)	(Benson & Axworthy, 1965)
k_{13} cm^3 sec^{-1}	2.3×10^{-15}	5.6×10^{-11} exp (-285/T)	(Benson & Axworthy, 1965)

The total rates of dissocation of 0_2 by solar UV-radiations and auroral electrons are given by J_2 and J_3 for 0_2 and 0_3. The expression for the particle dissociation rate is given by (3.5). The photodissociation rate is

$$J_{pi}(z) = \sum_{\lambda} \sigma_{i\lambda} Q_{\infty\lambda} \exp(-\tau_{\lambda}) \ (sec^{-1})$$

$\sigma_{i\lambda}$ is the cross section for dissociation as a function of wavelength for a particular constitutent oxygen (i = 2) and ozone (i = 3). Q_{∞} is the intensity of solar radiation outside the earth's atmosphere in units of photons cm^{-2} sec^{-1} unit wavelength^{-1}. The optical depth τ_{λ} represents the product of the absorption cross section and total number of absorbing molecules between height z and the sun and is a function of time.

The resulting differential equations are solved with the aid of a computer. Since some of the reactions are too fast to permit stable integration by the Runge-Kutta method, a more stable linearized finite difference scheme has been utilized in the present computation as shown in Appendix B.

4.2 Vertical Distributions of O_3 and in the Mesophere

4.2.1 In the Equatorial Region

In Figure 10, the diurnal variation of atomic oxygen, [O] in cm^{-3}, in the equatorial atmosphere at summer solstice is shown for each altitude from 50 km to 100 km at 10 km intervals. The variation of the vertical distribution of atomic oxygen as a function of altitude with time as a parameter is given in Figure 11, where increasing phase and decreasing phase of the variation are presented separately, i.e., (a) for morning (increasing phase), (b) for afternoon (decreasing phase). Figure 12 shows the variations of ozone at each altitude corresponding to the oxygen atom variations shown in Figure 10. The variation of vertical ozone distribution with time as a parameter is given in Figure 13, where the increasing phase, which starts after the sunset and the decreasing phase after the sunrise are shown separately in (a) and (b), respectively.

Comparisons with observations and with other calculations are shown in Figure 14, i.e., (i) Four cases of Hunt's (1966) results for the daytime equilibrium and pre-dawn maximum. The one with respect to a pure oxygen atmosphere (dash-dot line) and the other with respect to an oxygen-hydrogen atmosphere, (dashed line), (ii) Data of Rawcliffe, et al. (1963) obtained from satellite measurements of solar ultraviolet attenuation at twilight and from daytime rocket measurements reported by Johnson et al. (1954) (heavy lines). (iii) theoretical results for night time distribution given by Nicolet (10^4 sec after sunset, 1958) and by Horiuchi ($3 \cdot 10^4$ sec after sunset, 1961) (dotted lines), and (iv) nighttime of data, Reed and Scolnik (1964) obtained by UV-starlight measurements by rocket (circles) and night time data given by Mikirov (1965) obtained by UV-moon light measurements by rocket (dot with horizontal bar).

As can be seen, Figure 14, there is reasonable agreement between daytime observations and Hunt's calculation for daytime distribution with respect to the oxygen-hydrogen atmosphere between 50 km and 80 km. Although Hunt's conclusions that the use of a pure oxygen atmosphere leads to the too large ozone concentration can be also confirmed by the present calculation for the altitude below 80 km, his equilibrium (daytime) ozone distribution above 80 km level is too large. It should be noted that oxygen atom concentration above 90 km used by Hunt (1966) is nearly one order of magnitude high as compared to the recent direct measurements (Golomb et al. 1965).

On the other hand, night time enhancement of mesospheric ozone with a maximum around 70 km obtained by present calculation and by Hunt's pure oxygen atmosphere results show better agreement with observation than oxygen-hydrogen atmosphere results. Since the data of Reed and Scolnik require some

corrections for the spectrum-line widths with altitude (Reed, 1966), detailed comparison with data seems premature. It should be noted, however, that Mikirov's observation indicates far larger night time enhancement than present estimation and rather agree with Nicolet's and Horiuchi's estimations. Further night time mesospheric ozone measurements are necessary to discuss these differences. It has been noted that below 80 km the night time ozone concentrations are unaffected by hydrogen reactions since in the absence of sunlight the free hydrogen concentration falls to insignificant values. Therefore, unless there is significant dissociation of water vapor by electron impact, a pure oxygen atmosphere should be a sufficiently good approximation for use in describing auroral events occurring at night.

From Figure 10, 11, 12 and 13, the relaxation time of atmospheric oxygen atom, τ_1 (in sec), and that of ozone τ_3 (in sec) can be obtained for the temperature independent rate coefficients of Table 3. They are shown in Fig. 15 comparing with Hunt's results (1964).

4.2.2 In the Polar Region

Because of conditions of prolonged twilight, the distribution of constituents in the polar winter mesosphere is particularly difficult to describe. In Fig. 16(a) and (b) corresponding for the solar declination $\delta = 0°$ (equinox) and $\delta = -10°$, respectively. On this basis one would expect very low atomic oxygen concentration in the winter polar mesosphere, if there is no subsidence and horizontal transport from the sun-lit latitudes. In 1951, Kellogg and Schilling considered adiabatic heating due to air-subsidence at least at the rate of 1 km/day in an effort to

explain the increase in temperature of the winter mesosphere which is warmer than that in summer. Later Kellogg (1961) suggested that atomic oxygen created at heights above 80 km would be carried polewards to the dark hemisphere, where subsidence of the oxygen would increase the heating rate by the exothermic (5.08 eV) three body recombination reaction. Young and Epstein (1962) have shown that rates of subsidence of 0.2 cm/sec are sufficient to account for the observed heating provided the atomic oxygen concentration at 115 km is 1.5×10^{11} cm^{-3} or greater. On the basis of this density, it was shown that atomic oxygen densities of the order of 10^{12} cm^{-3} can be obtained at 70 km. The value of the rate coefficient which was chosen for k_{13} in this calculation is, however, one order of magnitude larger than that utilized by Hunt (1966). It is also possible for diffusion to be active in redistributing the atomic oxygen concentration and ozone formed in the upper mesosphere and in the lower thermosphere the effect of diffusion is estimated in Appendix C.

5. MESOSPHERIC OXYGEN DISTRIBUTION DURING AURORAL EVENTS

In Figure 9, the dissociation rates per incident electron have been given for two exponential spectra for e-folding energies, E_a = 5 kev and 100 kev. These spectra represent the limits for soft and hard spectrum of observable auroral electrons and can be used to establish the particle flux necessary to modify the atomic oxygen distribution in each instance.

Such an estimate can be made by employing the time independent solution of equation 4.2 and solving for the flux necessary to overcome the decay terms. As can be seen from Figure 9, a spectrum with E_a = 5 kev can have no effect at altitudes of 80 km and below. On the other hand, if a flux is more than 5×10^5

electrons/cm^2 sec, then the production rate can overcome recombination effects at 70 km for the E_a = 100 kev case. It is, therefore, the hard spectrum events that are of importance in modifying the atmosphere below 80 km, where atomic oxygen has a short lifetime (see Figure 15). Most bright auroras are, however, not of this hard spectrum type but are characterized by the soft spectrum with E_a's of 5 to 10 kev and by the fluxes of 10^9 to 10^{12} electrons/cm^2 sec. (McIlwain, 1960; Brown, 1966). Such events are not important unless the duration is of the order of several hours which might affect the atomic oxygen distribution above 80 km level, since the lifetime of atomic oxygen is long above these altitudes. Hard spectrum events of the type sufficient to affect the atomic oxygen concentration have been reported by Bailey et al., (1966) on the basis of forward-scatter radio-propagation data and balloon measurements of auroral bremsstrahlung. (Brown, 1966). Such events referred to as relativistic electron precipitation events, or 'REP's, appear to be characterized by E_a's between 60 and 150 kev and fluxes between 10^6 and 2×10^4 electrons/cm^2 sec. There is also satellite evidence of hard spectra auroral electrons. (Mann et. al., 1963).

In the present calculation, equations (4.1)-(4.3) are solved by the method described previously (and shown in Appendix B) for a latitude of 70° during equinox. In addition to the small solar photodissociation rate, particle fluxes are superimposed. As stated previously the cross-section of O_3 dissociation by electron impact is not known. However, the dissociation cross section of ozone, which is a triatomic molecule, by electron impact should be larger than that of the diatomic molecule. Therefore, two values have been assigned to the ozone dissociation rate, i.e., $J_3 = 10^2 J_2$ and $J_3 = J_2$. It will be shown that the effect

of auroral events on the temporal and spatial variations of atmospheric ozone and oxygen are not drastically affected by the assumption of the O_3 - dissociation rate unless it is assumed to be unreasonably small.

The following eight cases have been considered in the calculations; (i) Flux (intensity) of impinging auroral electrons $i_0 = 10^{11}$ to $i_0 = 10^5$ (cm^{-2} sec^{-1}). (ii) Energy spectrum of auroral electrons

$$j(E_0) = j_0 \exp\left(-\frac{E_0}{E_a}\right)$$

where E_a = 100 kev (hard spectrum) and E_a = 5 kev (soft spectrum). (iii) Ratio of dissociation rate of O_2 and of O_3, $J_3 = J_2 \times 10^2$ and $J_3 = J_2$. Duration of auroral bombardment was assumed to be 10 minutes, initiated at midnight for all calculations.

It was found that the soft spectrum case had essentially no effect even for large fluxes of incident electrons. Hard spectrum events of even short duration (1 minute or so) can give rise to significant enhancements at low altitudes. For instance for a flux of 10^5 electrons/cm^2 sec. a density 10^5 cm^{-3} atomic oxygen can be maintained at night at 60 km and for the same flux the density at 70 km can reach densities of 10^8 cm^{-3}. The resulting atomic oxygen and ozone distributions for the hard spectrum case (E_a = 100 kev) are shown in Fig. 17 (a-c) and 18 (a-c) for $J_3 = J_2 \times 10^2$ and $J_3 = J_2$, respectively, for the extreme case of $i_0 = 10^{11}$ cm^{-2} sec^{-1}.

From these figures, it can be seen that the atomic oxygen concentration is altered significantly below 80 km. In fact there is an increase of five orders of magnitude at 70 km, which decays with time constant τ_1 indicated in Fig. 15.

The increase in ozone $[O_3]$ is most significant around the 60-70 km level and is almost independent of the assumed ozone dissociation rate unless this is chosen to be negligibly small. From the foregoing, it is evident that for a hard spectrum auroral electron (E_a = 100 kev) and large incident flux (i_0 = 10^{11} cm^{-2} sec^{-1}), the profiles of atomic oxygen and to a lesser extent of ozone are substantially modified during and after the period of electron precipitation. Since the diffusion time of dissociated oxygen is long at these altitudes, the enhancement is confined within the horizontally narrow domain of particle precipitation (within bright auroras).

From the present calculation, we can see that the effect of O_2 dissociation is significant only below 80 km level for both processes of dissociations, i.e. by auroral particles as well as by solar UV-radiation. Since no auroral electrons with energy less than 100 kev penetrate below this level (Fig. 8), the rate of auroral dissociation depends strongly on the amount of high energy electron or on the spectrum of auroral electrons. In other words, if the spectrum is soft as seen in most bright auroras (McIlwain 1960, Brown 1966), no effects of auroral dissociation can be detected. On the other hand, if the spectrum is hard, increase of atomic oxygen below the 80 km level together with a subsequent increase of mesospheric ozone can occur. It should be noted, however, that hard spectra of auroral electrons appear generally in weak displays (Brown 1966). Durations should be, therefore, more than hours before the effects of auroral dissociation of atmospheric oxygens can be observable.

If local variations of auroral activities are considered, the intensity of auroral electron, its spectra change drastically within milli-seconds and several hundreds meters of horizontal scale (O'Brien, 1964, Brown, 1966, Mozer and

Bruston, 1966). The time constants of oxygen allotrope variations above stratosphere are, however, at least the order of minutes (Fig. 15). The intensities and spectra of auroral electrons to be compared to the present calculation are, therefore, those averaged over several minutes and many hundreds of kilometers in horizontal scale. In this respect, auroral effects on atmospheric oxygen are quite similar to those deduced from the auroral absorption measurements by riometer as far as time and horizontal scales are concerned.

Finally, the following can be regarded as one of the important differences between the effects of solar UV-radiations and those of auroral particles on the atmospheric oxygen; i.e., in the case of solar ultra-violet dissociation, the increase of atomic oxygen is always accompanied by the decrease of ozone, while both oxygen atoms and ozone increase in the case of auroral dissociation. This is essentially due to the steep spectrum of solar UV-radiation in which the intensity of Schumann-Runge region is nearly three orders of magnitude less than those ozone-destructing Hartley regions.

According to Akasofu (1964), the input energy flux of auroral particle is of the order of 80 ergs/cm^2 sec (the total energy deposit-rate, 8×10^{16} ergs/sec, divided by the total cross-sectional area exposed to incoming auroral electron, 10^{15} cm^2). This figure is comparable to the energy flux of solar UV-radiation with wave length shorter than 2000 Å (Hinteregger, 1965). It should be noted, however that the energy flux of bright aurora exceeds this figure more than several orders of magnitude, fluctuating within the order of milli-seconds.

6. IONOSPHERIC EFFECTS OF OZONE AND ATOMIC OXYGEN ENHANCEMENT

When an auroral electron interacts with the atmosphere, it loses the majority of its energy through excitation and ionization. The resulting ionization leads to increased radio wave absorption during auroral electron precipitation and in the case of proton flares polar cap absorption events. An adequate description of these events depends on a knowledge of the electron distribution which is dependent on the negative ion distribution in the D region. The species of negative ion is unknown at present. However, it is usual to assume O_2^- although O_3^- and NO_2^- have been suggested. The negative ion is formed initially by electron attachment. The species of negative ion may then be changed by charge transfer reactions or the ion may be destroyed by a variety of processes. These include the very important associative detachment reaction

$$O_2^- + O \rightarrow O_3 + e \qquad (6.1)$$

This reaction has figured in practically every theoretical treatment of the lower ionosphere both for the normal diurnal variation Aiken (1962) and for disturbed events such as PCA's Whitten and Poppoff (1962) Reid (1966). Associative detachment was also utilized to explain auroral absorption events by Aikin and Maier (1963) who suggested that a modification of the atomic oxygen distribution by the incoming energetic particle might change the negative ion density profile during such events.

Fehsenfeld, et al. (1966) have recently measured the rate of (6.1) and obtained a value of 3×10^{-10} cm^{-3} sec^{-1} which is more than sufficient to

make this process dominant above photodetachment during the day. If only O_2^- is considered the negative ion distribution will be controlled entirely by the atomic oxygen concentration.

However, the possibility that O_2^- and O^- may charge exchange with neutral species to form ions such as O_3^- and NO_2^- must be given consideration. Ferguson (1966) has measured the rate of the reaction

$$O_3^- + CO_2 \rightarrow CO_3^- + O_2$$

and found it to have a rate of 3×10^{-10} cm^{-3} sec^{-1} so that ions of this species are a possibility as well as

$$O_3^- + NO \rightarrow NO_3^- + O$$

It is evident that the distribution of O and O_3 can greatly influence the ionosphere wherever negative ions are of importance. The possibility exists that the negative ion distribution and perhaps the species is quite different between the normal D region, that affected by hard spectrum auroral electrons and polar cap protons, simply because the distribution of ozone and atomic oxygen differs in the lower mesosphere during these circumstances.

7. CONCLUSIONS

The time dependent photochemical equations describing the vertical distribution of ozone and atomic oxygen in a pure oxygen atmosphere have been solved for the equatorial and polar regions. The extended periods of twilight play an important role in the polar regions. Continuous sunlight can lead to an excess of atomic oxygen at altitudes where the lifetime is greater than one day. For winter

periods when the insolation is absent and appreciable atomic oxygen concentration cannot be maintained at altitudes below 80 km, without a downward flow mechanism such as subsidence or diffusion or a production mechanism such as a large flux of energetic electrons.

It has been shown that the cross section for molecular oxygen dissociation by low energy electrons is quite large (Fig. 3). Thus secondary electrons created during auroral particle precipitation into the atmosphere can modify the atomic oxygen and ozone distribution. If the energy spectrum of the auroral primary electrons is very hard such that the e-folding energy E_a is 50 kev or greater, mesospheric ozone and atomic oxygen concentrations around 60 - 70 km increases significantly (Fig. 17-20). The majority of events are not of this type but are generally very soft and rather monoenergetic with energy range 10 - 50 kev. For events of this type there is no modification of the atmosphere unless the event is of such a long duration as to increase the atomic oxygen concentration above 90 km. Therefore, significant enhancement of mesospheric ozone during auroral activity (Murcray 1957) seems very unlikely in general although it may occur for special events. Most of the UV-emissions from excited nitrogen molecules originating from auroral electron bombardments are in the far ultraviolet regions, which exceed the ionization threshold of molecular oxygen. Therefore, the auroral UV-emissions lead to 0_2-ionization rather than 0_2-dissociation (Green and Barth 1965) and will not affect present results.

APPENDIX A

Analytic Formula for $i(E, E_0, x)$

The number of electrons whose energy is between E and $E + dE$ (in keV) at the atmospheric depth x ($g\ cm^{-2}$), corresponding to monoenergetic vertically incident electrons with energy E_0, $i(E, E_0, x)$ has been calculated by means of the Monte Carlo method (Maeda, 1965). This can be approximated by

$$i(E, E_0, x) = \frac{Ae^{-a(\xi+\xi_0)^b}}{N(E_0, x)} i_0(E, E_0, x) \tag{A-1}$$

where

$$a = 4.42, \quad b = 2.8, \quad A = 1, \quad \xi_0 = 0.$$

and

$$i_0(E, E_0, x) = E_0^{n(\xi)-1} \left[\frac{(1-y)}{(1-y_m)^{0.1}}\right]^{n(\xi)} \exp\left[-\left[\frac{1-y}{(1-y_m)^{0.9}}\right]^{n(\xi)}\right]$$

$$\xi = x/r_0, \quad y = E/E_0, \quad y_m = E_m/E_0 \tag{A-2}$$

$$r_0 = 4.57 \cdot 10^{-6} E_0^{7/4} \tag{A-3}$$

$$E_m = [(r_0 - x)/r_0]^{4/7} \tag{A-4}$$

and

$$N(E_0, x) = \int_0^{E_0} i_0(E, E_0, x)\, dE$$

$$= E_0 \int_0^1 i_0(y, 1, x)\, dy$$

The empirical formula for a range r_0 ($g\ cm^{-2}$) of electrons with initial energy E_0 (keV) in air shown by Eq. (A-3) Grün (1957) and E_m given by Eq. (A-4) corresponds to the residual energy of electrons at the depth x in air.

Since the integrand $i(y, 1, x)$ is independent of E_0, the normalization factor of Eq. (A-1), $N(E_0, x)$ is written as:

$$N(E_0, x) = E_0 \int_0^1 i_0(y, x)\, dy \qquad \text{(A-5)}$$

where

$$i_0(y, x) = \left[\frac{(1-y)}{(1-y_m)^{0.1}}\right]^{n(\xi)} \exp\left[-\left(\frac{1-y}{(1-y_m)^{0.9}}\right)^{n(\xi)}\right] \qquad \text{(A-6)}$$

Numerical values of (A-6) for E_0 = 20 keV are shown in Fig. 6, with comparison to Monte Carlo results (Maeda, 1965 a,b).

Another term in Eq. (A-1), $Ae^{-(\xi+\xi_0)^b}$ is an empirical expression of total intensity of vertically incident monoenergetic electron E_0, at the depth $x = \xi \cdot r_0$, which has been also computed by Monte Carlo method (Maeda, 1965). Comparisons of numerical values of this factor and Monte Carlo results are shown in Fig. 7.

APPENDIX B

Integration of the Differential Equations by Finite Difference Method

The differential equation (4.1) can be replaced with the following finite difference scheme;

$$\dot{0}_3 \simeq \frac{0_3^{(n+1)} - 0_3^{(n)}}{\Delta t} \tag{B-1}$$

$$= 0_1^{(n)} \left[k_{12} \cdot M \cdot 0_2^{(n+1)} - k_{13} \cdot 0_3^{(n+1)} \right] - J_3 \cdot 0_3^{(n+1)}$$

where 0_i , $\dot{0}_i$ stand for $[0_i]$ and $\frac{d[0_i]}{dt}$ in Eq. (4.1), and the superscripts n, $n+1$ refer to the time t_n and $t_{n+1} = t_n + \Delta t$, respectively.

Similarly, Eq. (4.2) can be replaced by

$$\dot{0}_1 \simeq \frac{0_1^{(n+1)} - 0_1^{(n)}}{\Delta t} \tag{B-2}$$

$$= 2 J_2 \cdot 0_2^{(n+1)} + J_3 \cdot 0_3^{(n+1)} + 0_1^{(n)} \left[-2k_{11} \cdot M \cdot 0_1^{(n+1)} - k_{12} \cdot M \cdot 0_2^{(n+1)} - k_{13} \cdot 0_3^{(n+1)} \right]$$

Corresponding to the reactions listed in Table 2, time variation of 0_2 can be also written as;

$$\dot{0}_2 \simeq \frac{0_2^{(n+1)} - 0_2^{(n)}}{\Delta t}$$

$$= 0_1^{(n)} \left[k_{11} M 0_1^{(n+1)} + 2k_{13} 0_3^{(n+1)} \right] \tag{B-3}$$

$$- 0_2^{(n+1)} \cdot \left[k_{12} M 0_1^{(n+1)} + J_2 \right] + J_3 \cdot 0_3^{(n+1)}$$

This equation can be also derived by Eq. (4.1) and Eq. (4.2) with a condition for conservation of oxygen allotrope at each layers, i.e.,

$$3\,[O_3] + 2\,[O_2] + [O_1] = \text{const.}$$

or (B-4)

$$\dot{O}_2 = \frac{-1}{2}\,[\dot{O}_1 + 3\,\dot{O}_3]$$

It should be noted that the equations (B-1), (B-2) and (B-3) are written in linear form which can be simplified by writing in matrix, i.e.,

$$\begin{pmatrix} O_1^{(n)} \\ O_2^{(n)} \\ O_3^{(n)} \end{pmatrix} = \begin{pmatrix} 1 + O_1^{(n)} \cdot 2k_{11}M\Delta t & (O_1^{(n)}k_{12}M - 2J_2)\Delta t & (O_1^{(n)}k_{13} - J_3)\Delta t \\ -O_1^{(n)}k_{11}M\Delta t & 1 + (O_1^{(n)}k_{12}M + J_2)\Delta t & -(O_1^{(n)}2k_{13} + J_3)\Delta t \\ 0 & -O_1^{(n)}k_{12}M\Delta t & 1 + (O_1^{(n)}k_{13} + J_3)\Delta t \end{pmatrix} \begin{pmatrix} O_1^{(n+1)} \\ O_2^{(n+1)} \\ O_3^{(n+1)} \end{pmatrix}$$

By means of matrix inversion $O_i^{(n+1)}$'s are easily obtained by knowing $O_i^{(n)}$'s, starting from certain initial conditions. As can be seen from (B-1) and (B-3) replacement of original differential equations (4.1), (4.2) by the finite difference schemes are not unique. It should be noted, however, that partial replacements such as $O_i^{(n+1)} \cdot O_i^{(n+1)}$ by $O_i^{(n)} \cdot O_i^{(n+1)}$ are essential to retain the linearity of the scheme by which integral stability in numerical integrations is easily to be achieved.

The present method works for $\Delta t = 20$ sec for all altitudes 50 - 150 km and seems progressively unstable below 50 km for $\Delta t = 20$ sec, which can be extended, however, by reducing Δt.

APPENDIX C

Effect of Diffusion

The diffusion of neutral atoms and molecules in the upper atmosphere can be described in terms of molecular diffusion and eddy diffusion, both of which depend on the vertical gradients of densities, pressures and temperatures in the atmosphere. Calculations on these effects have been made by several investigators (Mange 1954; Colegrove, et al., 1965; Shimazaki, 1966). Numerical computations including these effects into present calculation are not impossible but increases complications and correspondingly machine time. Prior to including such processes, the effects of diffusion can be estimated. Since the products of O_2-dissociation have a finite life time in the atmosphere, which changes with altitude, one can define the effective diffusion length of these elements by

$$\ell_i(z) = [D_i(z) \cdot \tau_i(z)]^{1/2}$$

where

$D_i(z)$'s are the diffusion coefficients for O_i at the altitude z km, in cm^2 sec^{-1}, and

$\tau_i(z)$'s are the life time of O_i in the atmosphere at the altitude z km, in second, which are shown in Fig. 15.

It is known that above a certain altitude (turbopause) the molecular diffusion coefficient exceeds the eddy diffusion coefficient and increases further with altitude. Since the present calculation is an order of magnitude estimation, $D_i(z)$'s are taken from the corrected value given by Johnson and Wilkinson (1965). If $\ell_i(z)$ is less than the local vertical scale for gradient, $h_i(z)$, of the element O_i at z in km,

the effects of diffusion can be regarded as unimportant, while if $\ell_i(z)$ exceed $h_i(z)$, diffusion is important to consider in finding the vertical distribution of elements O_i in the atmosphere around the altitude z. The results are shown in the following table;

TABLE 3
The Effective Diffusion Length, ℓ_i (in km) and the Local Vertical Scale for Gradient, h_i (in km) in the Mesosphere, Where Suffix i = 1, 3 Stand For Atomic Oxygen and Ozone, Respectively

Altitude z in km	ℓ_1 (oxygen atom)	h_1 (oxygen atom)	ℓ_3 (ozone)	h_3 (ozone)
50	0.06	1.	0.22	5.0
60	0.1	3.	.50	6.5
70	0.35	6.	.27	5.0
80	1.8	12	.18	4.5
90	8.7	21.	.08	4.0
100	120.	∞	.054	3.5
110	3600	13	.036	3.0
120	$>10^5$	20	.020	3.0

From this table, we can conclude that the diffusion is not important to determine the vertical distributions of atomic oxygen and ozone below 90 km but cannot be disregarded above 100 km level. As can be seen from Fig. 15, the effect of diffusion is not as important for the ozone distribution as for that of atomic oxygen.

BIBLIOGRAPHY

Aikin, A. C., "A Preliminary Study of Sunrise Effects in the D Region" in Electron Density Profiles in the Ionosphere and Exosphere, Ed. B. Maehlum, Bergman Press, 1962.

Aikin, A. C. and Maier E., "The Effect of Auroral Bremsstrahlung in the Lower Ionosphere," NASA, GSFC X-615-63-114, April, 1963.

Akasofu, S. I., "A Source of the Energy for Geomagnetic Storms and Auroras," Planet Space Sci., 12, 801-833, 1964.

Bailey, D. K., M. A. Pomerantz, K. W. Sullivan and C. C. Taib, "Characteristics of Precipitated Electrons Inferred from Ionospheric Forward Scatter," J.G.R. 71, 5179-5182, 1966.

Barth, C. A., "Nitrogen and Oxygen Atomic Reactions in the Chemosphere," Chemical Reactions in the Lower and Upper Atmosphere, Interscience Publishers, New York, 1961.

Bates, D. and M. Nicolet, "The Photochemistry of Atmospheric Water Vapor," J.G.R. 55, 301-327, 1950.

Bauer, E., and C. E. Bartky, "Calculation of Inelastic Electron-Atom and Electron-Molecule Collision Cross Sections by Classical Methods," Aeronutronic Publication No. U-2943, Philco Corporation, 1965.

Benson, S. W. and A. E. Axworthy, "Reconsideration of the Rate Constants From the Thermal Decomposition of Ozone," J. Chem. Phys. 42, 2614-2615, 1965.

Branscomb, L. M., "A Review of Photodetachment and Related Negative Ion Processes Relevant to Aeronomy," Ann. Geophys. 20, 88-105, 1964.

Brown, R. R., "Feature of the Auroral Electron Energy Spectrum Inferred from Observations of Ionosphere Absorption," Arkiv, Geofys. 4, 405-426, 1964.

Brown, R. R., "Electron Precipitation in the Auroral Zone," Space Science Reviews, 5, 311-387, 1966.

Carver, J. H. and Horton, B. H. and F. G. Burger, "Nocturnal Ozone Distribution in the Upper Atmosphere," J. Geophys. Res., 71, 4189-4191, 1966.

Chamberlain, J. W., "Physics of the Aurora and Airglow," Academic Press Inc., N.Y., 1961

Chamberlain, J. W. and C. A. Smith, "On the Excitation Rates and Intensities of OH in the Airglow," J.G.R. 64, 611-614, 1959.

Chapman, S., "On Ozone and Atomic Oxygen in the Upper Atmosphere," Phil. Mag. 10, 369-383, 1930.

Chapman, S., "The Absorption and Dissociative of Ionizing Effect of Monochromatic Radiation in an Atmosphere on a Rotating Earth," Proc. Phys. Sco., 43, 26-45 (Part I), 483-501 (Part II), 1931.

Colegrove, F. D., W. B. Hanson and F. S. Johnson," Eddy Diffusion and Oxygen Transport in the Lower Thermosphere," J.G.R., 70, 4931-4941, 1965.

CIRA 1965, (Cospar International Reference Atmosphere 1965, Compiled by the members of COSPAR working group IV), North-Holland Pub. Co., 1965.

Dalgarno, A., "Corpuscular Radiation in the Upper Atmosphere," Ann. d. Geophys. 20, 65-74, 1964.

Ditchburn, R. W. and P. A. Young, "The Absorption of Molecular Oxygen between 1850 and 2500 A," J. Atm. Terr. Phys., 24, 127-139, 1962.

Dütsch, H. U., "Current Problems of the Photochemical Theory of Atmospheric Ozone," Proc. of Intn'l. Sympos. San Francisco, April 18-20, 1961. (Chemical Reactions in the Lower and Upper Atmosphere, Interscience Publishers, New York, 1961).

Evans, Davis S., "Rocket Observations of Low Energy Auroral Electrons," X-611-66-376, August 1966.

Fehsenfeld, F. C., E. E. Ferguson and A. L. Schmeltekopf, "Thermal Energy Association Detachment Reactions of Negative Ions," J. Chem. Phys. 45, 1844-1845, 1966.

Ferguson, E.E., private communication, 1966.

Frost, D. C. and C. A. McDowell, "The Ionization and Dissociation of Oxygen by Electron Impact," J. Am. Chem. Soc. 80, 6183-6187, 1958.

Gilmore, F. R., "Potential Energy Curves for N_2, NO, O_2 and Corresponding Ions," Rand Corporation Memorandum, RM-4034-PR, June 1964.

Glockler, G., and J. L. Wilson, "The Activation of Molecular Oxygen by Electron Impact," J. American Chemical Society, 54 (12), 4544-4558, 1932.

Golomb, D., N. W. Rosenberg, C. Aharonian, J. A. F. Hill and H. L. Alden," Oxygen Atom Determination in the Upper Atmosphere by Chem-iluminescence of Nitric Oxide," J.G.R. 70, 1155-1173, 1965.

Goody, R. M., "Atmospheric Radiation," I Theoretical Basis, Oxford Clarendon Press, London, 1964 (0^{16} 0^{16} - Pot Curve Fig. 3.15, p. 96)

Green, A. E. S. and C. A. Barth, "Calculations of Ultraviolet Molecular Nitrogen Emission from the Aurora," J.G.R. 70, 1083-1092, 1965.

Grün, A. E., "Lumineszenz-Photometrische der Energieabsorption in Strahlungsfeld von Elektronengnellen. Eindimensionale Fall in Luft," Zeit. Naturf, 12A, 89-95, 1957.

Gryzinski, M., "Classical Theory of Electronic and Ionic Inelastic Collisions," Phys. Rev. 115, 374-383, 1959.

Herzberg, G., "Molecular Spectra and Molecular Structure," D. Van Nostrand Co., Inc., 1950.

Hesstvedt, E., "On the Determination of Characteristic Times in a Pure Oxygen Atmosphere," Tellus 15, 82-88, 1963.

Hinteregger, H. E., "Absolute Intensity Measurements in the Extreme Ultraviolet Spectrum of Solar Radiation," Space Sci. Rev. 4, 461-497, 1965.

Horiuchi, G., "Odd Oxygen in the Mesosphere and Some Meteorological and Considerations," Geophysical Magazine, 30, 439-520, 1961.

Hultqvist, B., "Aurora," Goddard Space Flight Center (NASA) Report X-611-64-97, April 1964.

Hunt, B. G., "A Non-Equilibrium Investigation into the Diurnal Photochemical Atomic Oxygen and Ozone Variations in the Mesosphere," Tech. Note (Anstralian Research Establishment) PAD 82, February 1964.

Hunt, B. G., "Influence of Metastable Oxygen Molecules on Atmospheric Ozone," J.G.R. 70, 4990-4991, 1965.

Hunt, B. G., "The Need for a Modified Photochemical Theory of the Ozonosphere," J. Atmos. Soc., 23, 88-95, 1966a.

Hunt, G. B., "Photochemistry of Ozone in a Moist Atmosphere," J.G.R. 71, 1385-1398, 1966b.

Johnson, F. S., J. D. Purcell and R. Tousey, "Studies of the Ozone Layer over New Mexico" in Rocket Exploration of the Upper Atmosphere, Edited by R. Boyd and M. J. Seaton, p. 189, Pergamon Press, London, 1954.

Johnson, F.S. and E.M. Wilkins, Correction to 'Thermal Upper Limit on Eddy Diffusion in the Mesosphere and Lower Thermosphere', J.G.R. 70, 4063, 1965.

Kellogg, W. W., "Chemical Heating above the Polar Mesosphere in Winter," J. Meterol. 18, 373-381, 1961.

Kellogg, W. W. and G. F. Schilling, "A Proposed Model of the Circulation in the Upper Stratosphere," J. Met. 8, 222-230, 1951.

King, G. A. M., "The Dissociation of Oxygen and High Level Circulation in the Atmosphere," J. Atmos. Sci. 21, 231-237, 1964.

Lassettre, E. N., "Collision Cross Section Studies on Molecular Gases and the Dissociation of Oxygen and Water," Radiation Research, Supplement 1, 530-546, 1959.

Lassettre, E. N., S. M. Silverman and M. E. Krasnow, "Electronic Collision Cross Sections and Oscillator Strengths for Oxygen in the Schumann-Range Region," J. Chem. Phys., 40, 1261-1265, 1964.

Leovy, Conway, "Radiative Equilibrium of the Mesosphere," J. Atmos. Sci. 21, 238-248, 1964.

Maeda, K., "On the Heating of the Polar Upper Atmosphere," NASA Tech. Rept. R-141, 1962.

Maeda, K., "Auroral Dissociation of Molecular Oxygen in the Polar Mesosphere," J. Geophys. Res., 68, 185-197, 1963a.

Maeda, K., "On the Heating of Polar Night Mesosphere, Part I," Proceedings of the Int'l. Symp. on Strato-Mesospheric Circulation, (Aug. 1962), Met. Abhand, 36, 451-496, 1963b.

Maeda, K., "Diffusion of Loss Energy Auroral Electrons in the Atmosphere," J. Atm. and Terr. Phys., 27, 259-275, 1965a.

Maeda, K., "Diffusion of Auroral Electrons in the Atmosphere," NASA TN D-2612, February 1965b.

Maeda, K., and S. F. Singer, "Energy Dissipation of Spiraling Particles in the Polar Atmosphere," Arkiv f. Geophys., 3, 531-538, 1961.

Mann, L. G., S. D. Bloom and H. I. West, Jr., "The Electron Spectrum from 90 to 1200 kev as Observed on Discoverer Satellites 29 and 31," Space Research III, 447-462, 1963 (North-Holland Pub. Co.).

Mange, P., "The Diffusion and Dissociation of Molecular Oxygen in the Atmosphere above 100 Km," Scientific Report No. 64, Pennsylvania State Univ., 1954.

Massey, H.S.W., "Negative Ions," Cambridge University Press, 1950.

Massey, H.S.W., and E.H.S. Burhop, "Electronic and Ionic Impact Phenomena," The Oxford-Clarendon Press, 1956.

McDaniel, E. W., "Collision Phenomena in Ionized Gases," John Wiley and Sons, Inc., New York, 1964.

McGowan, J. W., E. M. Clark, H. P. Hanson, and R. F. Stebbings, Phys. Ref. Letters, 13, 620, 1964.

McIlwain, C. E., "Direct Measurement of Particles Producing Visible Auroras," J.G.R. 65, 2727-2747, 1960.

Mikirov, A. Y., "The Estimation of Ozone Concentration at the Heights of 44-102 km during night launches of Geophysical Rockets, Geomag. Aeronom., 5, 1120-1123, 1965 (NASA TT F-10, 006, July 1965).

Miller, D. E. and H. H. Stewart, "Observations of Atmospheric Ozone From an Artificial Earth Satellite," Proc. Roy. Soc., London, A288, 540-544, 1965.

Mozer, F. S. and J. P. Bruston, "Properties of the Auroral-Zone Electron Source Deduced from Electron Spectrums and Angular Distribution," J.G.R. 71, 4451-4460, 1966.

Murcray, W. B., "A Possible Auroral Enhancement of Infra-Red Radiation Emitted by Atmospheric Ozone," Nature, 180, 139 140, 1957.

Nicolet, M., "Aeronomic Conditions in the Mesosphere and Lower Thermosphere," Sci. Rept., April No. 102, 1958.

O'Brien, B. J., "High-Latitude Geophysical Studies with Satellite Injun 3," J.G.R. 69, 13-43, 1964.

Patzold, H. K., "The Photo-Chemistry of the Atmospheric Ozone Layer, Chemical Reactions in the Lower and Upper Atmosphere," 181-195, Interscience Pub., 1961.

Rapp, D., and D. D. Briglia, "Total Cross Sections for Negative Ion Formation in Gases by Electron Impact," Lockheed Missile and Space Co., Tech. Rept. 6-74-64-40, 1964.

Rapp, D., T. E. Sharp and D. D. Briglia, "On the Theoretical Interpretation of Resonance Dissociative Attachment Cross Sections," LMSC 6-74-64-45, 1964.

Rawcliffe, R. D., G. E. Meloy, R. M. Friedman and E. H. Rogers, "Measurement of Vertical Distribution of Ozone from a Polar Orbiting Satellite," J.G.R. 68, 6425-6429, 1963.

Reed, Edith, Private Communication, 1966.

Reed, Edith and Scolnik, Reuben, "A Nighttime Measurement of Ozone above 40 km," Goddard Space Flight Center X-613-64-267, 1964. (Presented in Intn'l. Ozone Symposium, Alburqurque, New Mexico, Sept. 1964).

Rees, M. H., "Auroral Ionization and Excitation by Incident Energetic Electrons," Planet. Space Science, 11, 1209-1218, 1963.

Reeves, R. R., G. Manella, and P. Harteck, "Rate of Recombination of Oxygen Atoms," J. Chem. Phys., 32, 632-633, 1960.

Reid, G. C., "Physical Process in the D-Region of the Ionosphere," Review of Geophys. 2, 311-333, 1964.

Reid, G. C., "Physics of the D-Region at High Latitudes," In Electron Density Profiles in the Ionosphere and Exosphere," North-Holland Publishing Co., Amsterdam, 1966.

Rossi, B., "High Energy Particles," Prentice Hall Inc., New York, 1952.

Schiff, H. I., "Reactions Involving Nitrogen and Oxygen," Ann. d. Geophys. 20, 115-127, 1964.

Schulz, G. J. and J. T. Dowell, "Excitation of Vibrational and Electronic Levels in 0_2 by Electron Impact," Phys. Rev. 128, 114-177-1962.

Shiff, H. I., and L. R. Megill, "The Influence of Metastable Oxygen Molecules on Ozone and Airglow," J.G.R. (Letters) 69, 5120-5121, 1964.

Shimazaki, T., "Dynamic Effects on Atomic and Molecular Oxygen Density Distributions in the Upper Atmosphere: A Numerical Solution to Equations of Motion and Continuity," Preprint 1966.

Silverman, S. M., and E. N. Lassettre, "Collision Cross Sections for Oxygen in the Excitation Energy Range 10 to 80 V," J. Chem. Phys., 40, 2922-2932, 1964.

Spencer, L. V., "Energy Dissipation by Fast Electrons," N.B.S. Monograph 1, 1959.

Tate, J. T. and P. T. Smith, "The Efficiencies of Ionization and Ionization Potential of Various Gases Under Electron Impact, Phys. Rev. 39, 270-273, 1932.

Thompson, J. B., "Electron Energy Distributions in Plasmas, VI Oxygen and Nitrogen, Proc. Roy. Soc. (London) A262, 503-528, 1961.

Wallace, L., "The OH Nightglow Emission," J. Atmos. Sci. 19, 1-16, 1962.

Watanabe, K., E. C. Y. Inn and M. Zelikoff, "Absorption Coefficients of Oxygen in the Vacuum Ultraviole," J. Chem. Phys. 21, 1026-1030, 1953.

Whitten, R. C. and I. G. Poppoff, "Associated Detachment in the D Region, J. Geophys. Res. 67, 1183, 1962.

Wu, C. S., "The Interaction of Beta Particles with Matter," in Nuclear Spectroscopy Part A., Ed. F. Ajzenberg-Selove, Academic Press, New York, 1960.

Young, C. and E. S. Epstein, "Atomic Oxygen in the Polar Winter Hemisphere," J. Atm. Sci. 19, 435-443, 1962.

FIGURE CAPTIONS

Figure 1. Potential energy curves of molecular oxygen.

Figure 2. Energy levels of the neutral oxygen atom.

Figure 3. Total cross sections of 0_2-dissociation by electron impacts. σ^-, σ_{SL} and σ_i stand for the reactions (2.1), (2.2) and (2.3), respectively. σ_M is the one used in the previous calculation corresponding to the reaction (2.2) (Maeda, 1962, 1963), whereas σ_{BB} is the one calculated by the classical theory for the reaction (2.2) (Bauer and Bartky, 1965).

Figure 4. The excitation spectrum of molecular oxygen by electron impact between 4 and 12 eV compared with optical absorption bands (Shulz and Dowell, 1962).

Figure 5. The number of secondary electrons per unit thickness of gas (0_2 and N_2, in g/cm^{-2}) per electron of energy E (in kev). The abscissa is electron energy in kev. Points marked by square and circle are taken from Tate-Smith (1932) and Wu (1960), respectively.

Figure 6. Comparison of $i(E, E_0, x)$ given by the formula (A-6) (dahsed lines) and that of Monte Carlo calculation for the vertically incident monoenergetic electrons of $E_0 = 20$ kev (full lines).

Figure 7. Variations of the total intensity of vertically incident monoenergetic electrons with atmosphere depth,

$$I(E_0 \xi) = \int_0^{E_0} i(E, E_0 \xi)\, dE$$

where

$$\xi = x/r_0, (r_0 = 9.824.10^{-4}\ g\,cm^{-2}\ \text{for}\ E_0 = 20\ keV)$$

Full line and dashed lines stand for the results of Monte Carlo calculation and empirical expression, (A-1), respectively. Another full line indicate the Monte Carlo result of variation of total energy flux of vertically incident monoenergetic electrons

Figure 8. Rate of 0_2-dissociation by monoenergetic auroral electrons (with energy E_0) as a function of altitude z (in km) for 5 kev $\leq E_0 \leq$ 1 Mev.

Figure 9. Rate of 0_2-dissociation by auroral electrons with energy e^{-E_0/E_a} vs. altitude z. Two curves correspond to E_a = 5 kev and E_a = 100 kev, respectively.

Figure 10. Diurnal variation of atomic oxygen (per cm^3) at each level from 50 km with 100 km with 10 km intervals in equatorial atmosphere at the summer solstice.

Figure 11. Diurnal variation of the vertical distribution of atomic oxygen with time as a parameter, where the increasing phase after sunrise, and decreasing phase of variation in the afternoon are shown separately in (a) and (b), respectively.

Figure 12. Diurnal variation of ozone at each level corresponding to the oxygen-atom variations shown in Fig. 10, in the equatorial atmosphere at summer solstice.

Figure 13. Vertical cross section of temporal variation of ozone shown in Fig. 12. To see the two phases of variation, the increasing and decreasing phases are shown separately.

Figure 14. Comparison of observed values and theoretical results of ionospheric ozone distributions at the daytime equilibrium and nighttime enhancement. (i) Full lines, present calculation, (ii) Dash-dot lines, Hunt's (1964) pure oxygen atmosphere results (iii) Dashed-lines, Hunt's (1966) oxygen-hydrogen atmosphere results (iv) Heavy lines, Rawcliffe et al. (1963) satellite observation and Johnson et al. (1958) rocket observation (v) Dotted lines, Nicolet's (1958) calculation for 10^4 sec after sunset and Horiuchi's (1961) calculation for 3.10^4 sec after sunset (vi) data points indicated by circles, Reed-Scolnik (1964) by UV-star light spectrum measurements (vii) data indicated by small dot with horizontal bar, Mikirov's (1965) data obtained by rocket observation of UV-moonlight attenuation.

Figure 15. Time constants of atmospheric oxygen-atom, τ_1 (in sec), and of ozone, τ_3 (in sec), with comparison with Hunt's (1966) results (dashed line).

Figure 16. Temporal variation of ozone and atomic oxygen in the polar hemisphere at the geographic latitude $\lambda = 70°$ (a) solar declination $\delta = 0°$ (equinox) and (b) $\delta = -10°$.

Figure 17. Variation of the 0 and 0_3 concentration during and after the hard spectrum electron precipitation (a) 60 and 70 km, (b) 80 and 90 km, and (c) 100, 110, and 120 km for $J_3 = J_2 \times 10^2$ and $i_0 = 10^{11}$ cm^{-3} sec^{-1}.

Figure 18. The same as Fig. 17 except $J_3 = J_2$.
(a) 60 and 70 km (b) 80 and 90 km (c) 100, 110 and 120 km.

Figure 19. Variation of vertical distribution of atomic oxygen due to the hard spectrum electron precipitation (a) during electron precipitation (increasing

phase) (b) after the cessation precipitation of $J_3 = J_3 \times 10^2$ and $i_0 = 10^{11}$ cm^{-2} sec^{-1}.

Figure 20. Variation of the vertical distribution of ionospheric ozone during and after hard spectrum electron precipitation for $J_3 = J_2 \times 10^2$ and $i = 10^{11}$ cm^{-2} sec^{-1}.

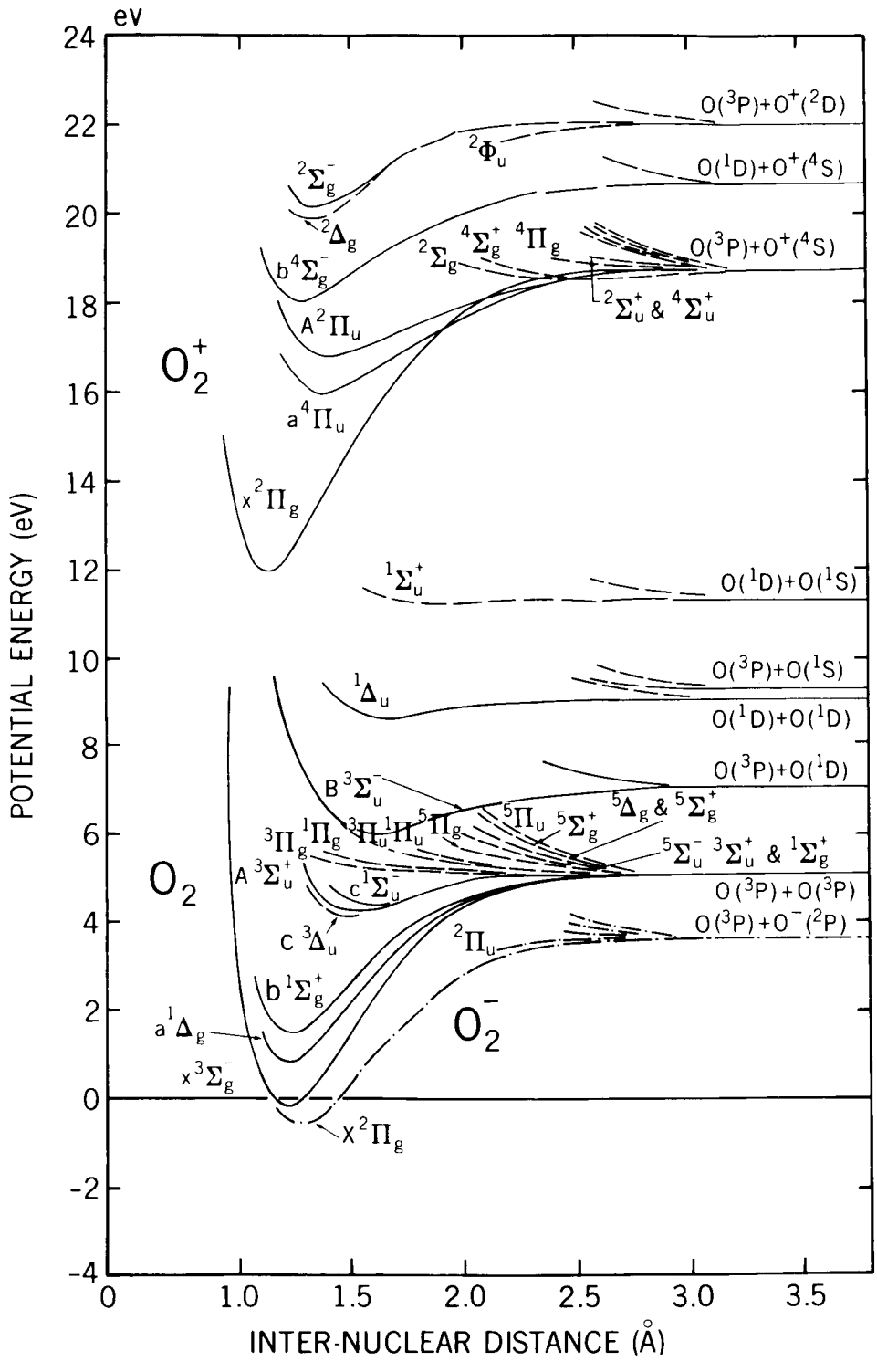

Figure 1–Potential curves of molecular oxygen.

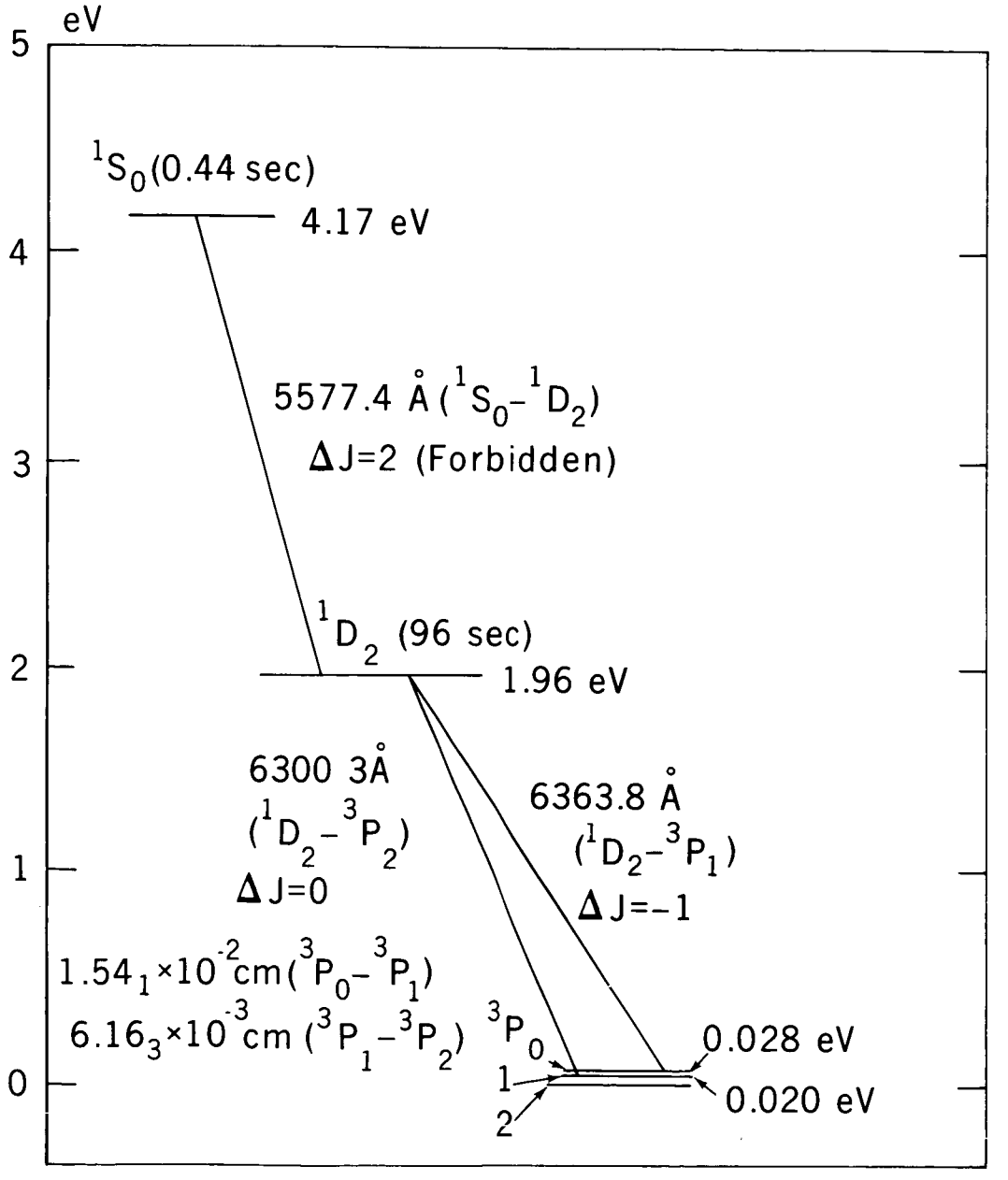

Figure 2–Energy levels of neutral oxygen atom.

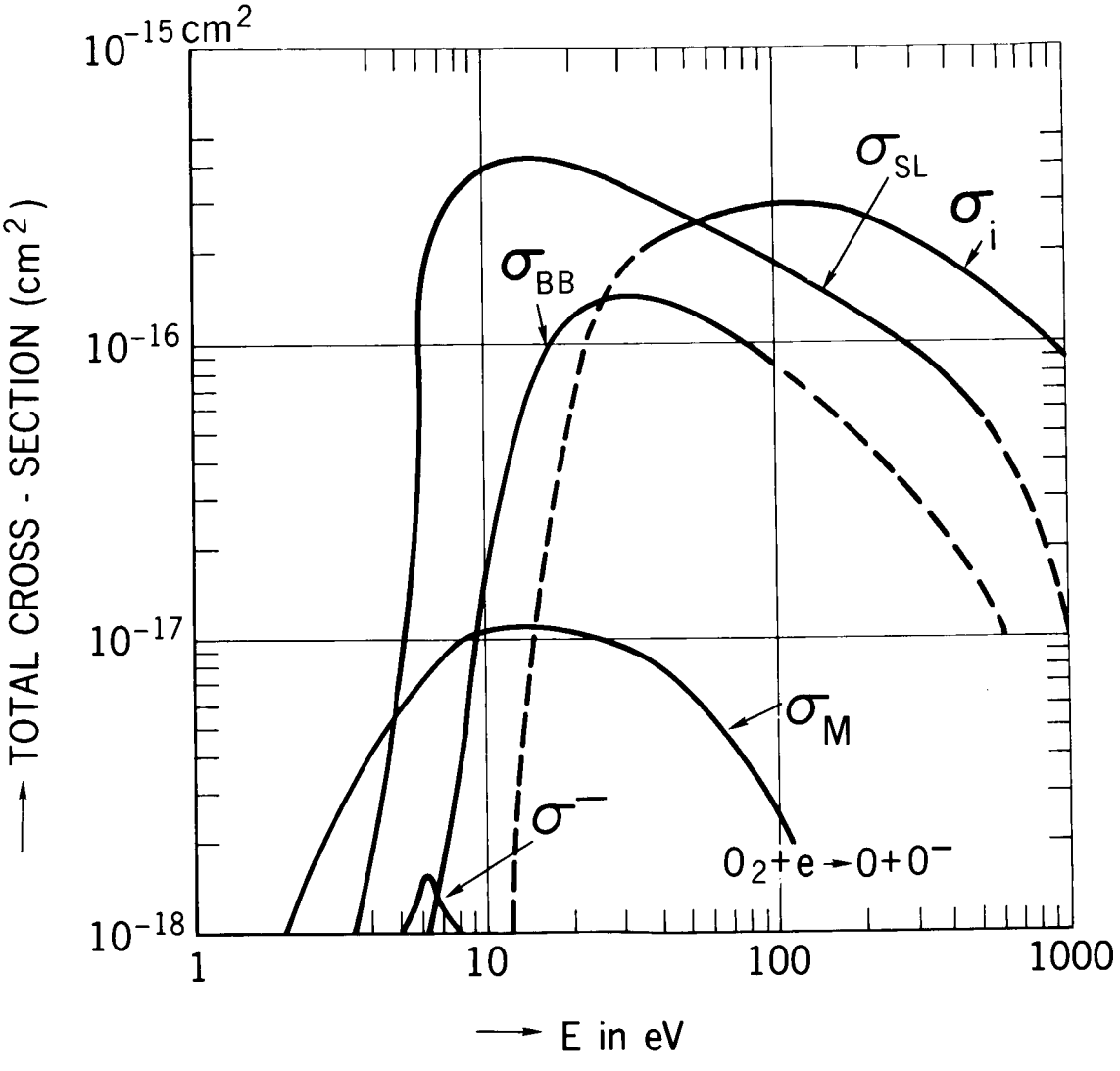

Figure 3–Total cross sections of O_2-dissociation by electron impacts. σ^-, σ_{SL} and σ_i stand for the reactions (2.1), (2.2) and (2.3), respectively. σ_M is the one used in the previous calculation corresponding to the reaction (2.2) (Maeda, 1962, 1963), whereas σ_{BB} is the one calculated by the classical theory for the reaction (2.2) (Bauer and Bartky, 1965).

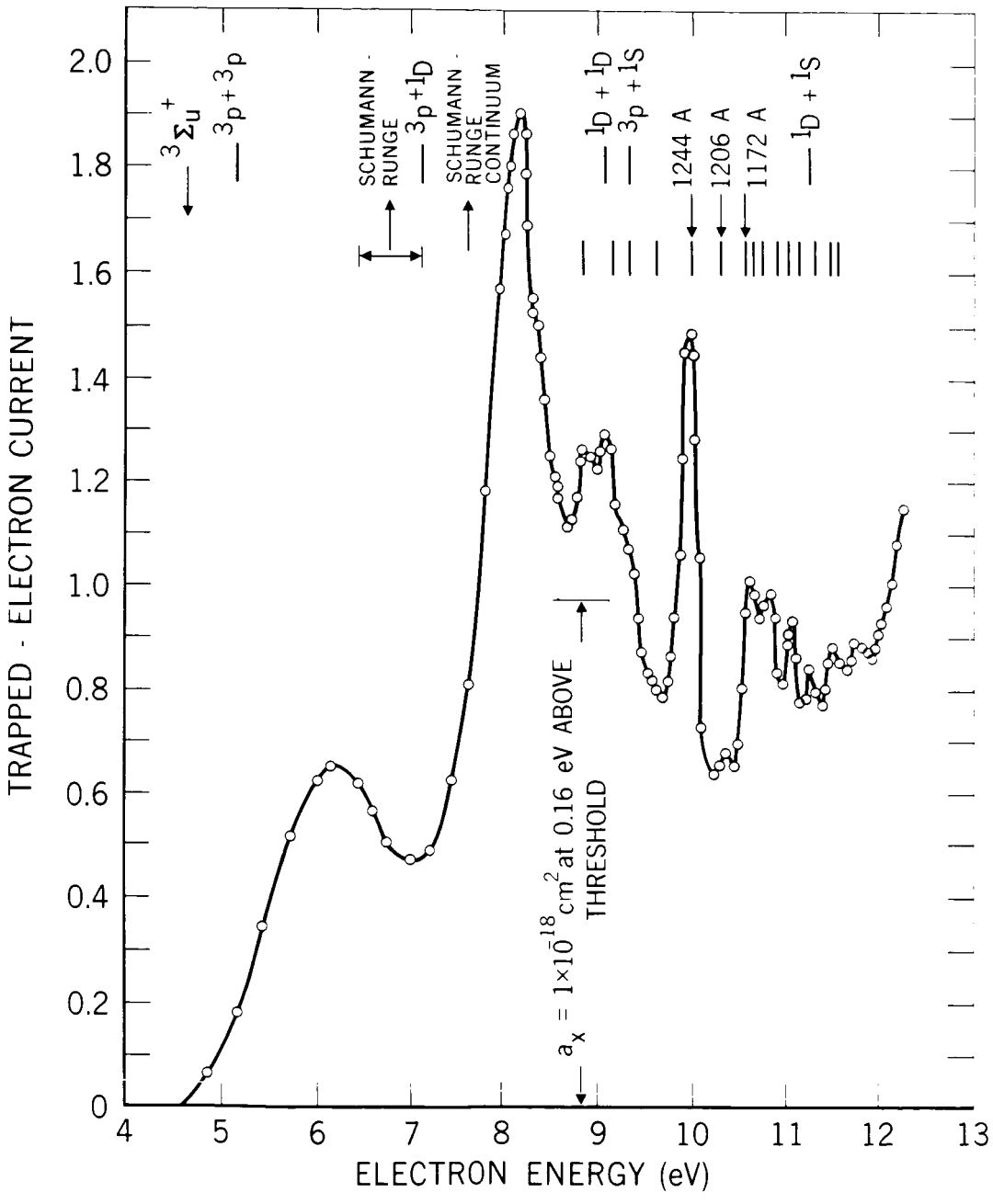
TRAPPED - ELECTRON CURRENT
ELECTRON ENERGY (eV)
$^3\Sigma_u^+$
$^3p + ^3p$
SCHUMANN - RUNGE
$^3p + ^1D$
SCHUMANN - RUNGE CONTINUUM
$^1D + ^1D$
$^3p + ^1S$
1244 A
1206 A
1172 A
$^1D + ^1S$
$a_x = 1 \times 10^{-18}$ cm^2 at 0.16 eV ABOVE THRESHOLD
0
0.2
0.4
0.6
0.8
1.0
1.2
1.4
1.6
1.8
2.0
4
5
6
7
8
9
10
11
12
13

Figure 4

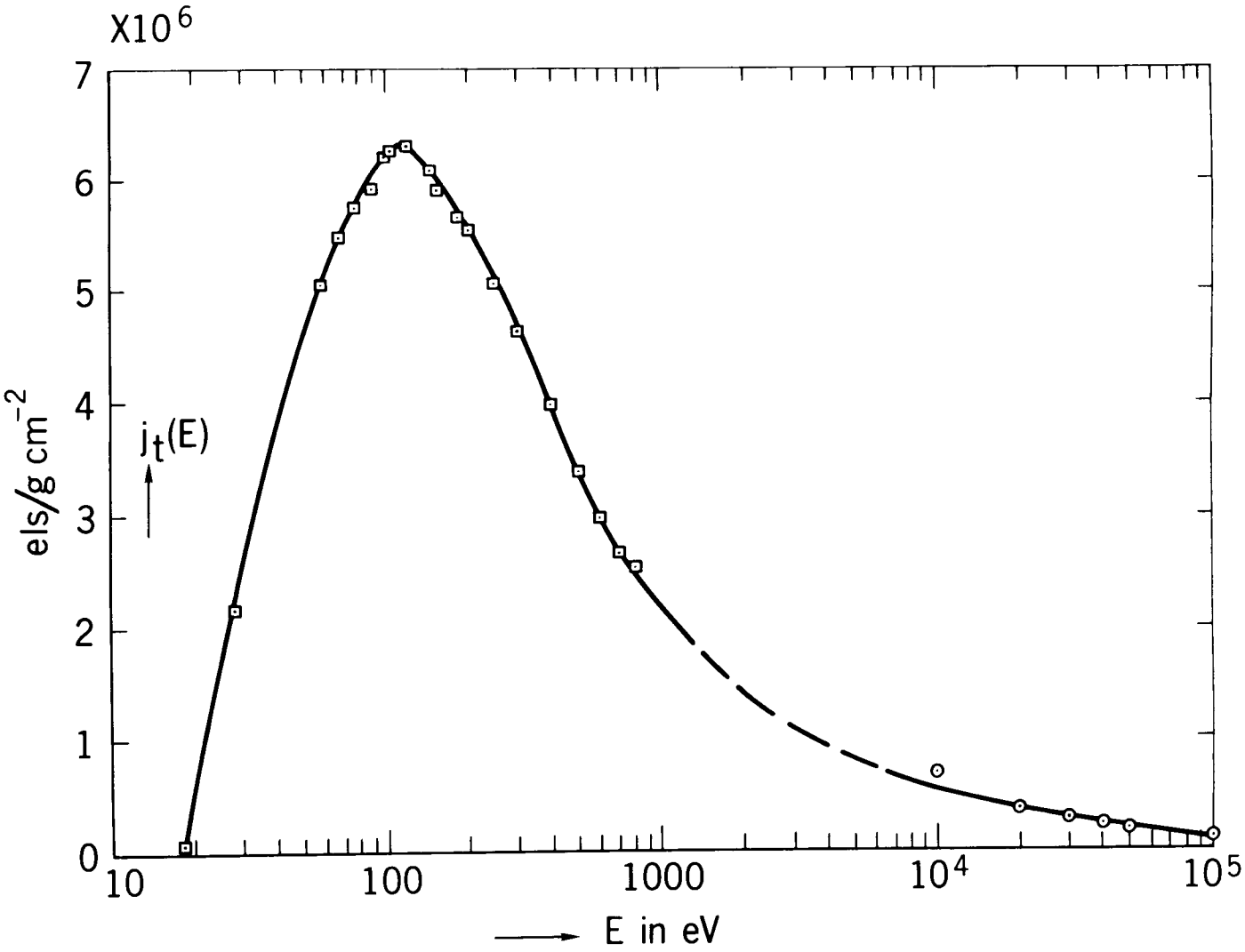

Figure 5–The number of secondary electrons per unit thickness of gas (0_2 and N_2, in g/cm^{-2}) per electron of energy E (in kev). The abscissa is energy of electron in kev. Points marked by square and circle are taken from Tate-Smith (1932) and Wu (1960), respectively.

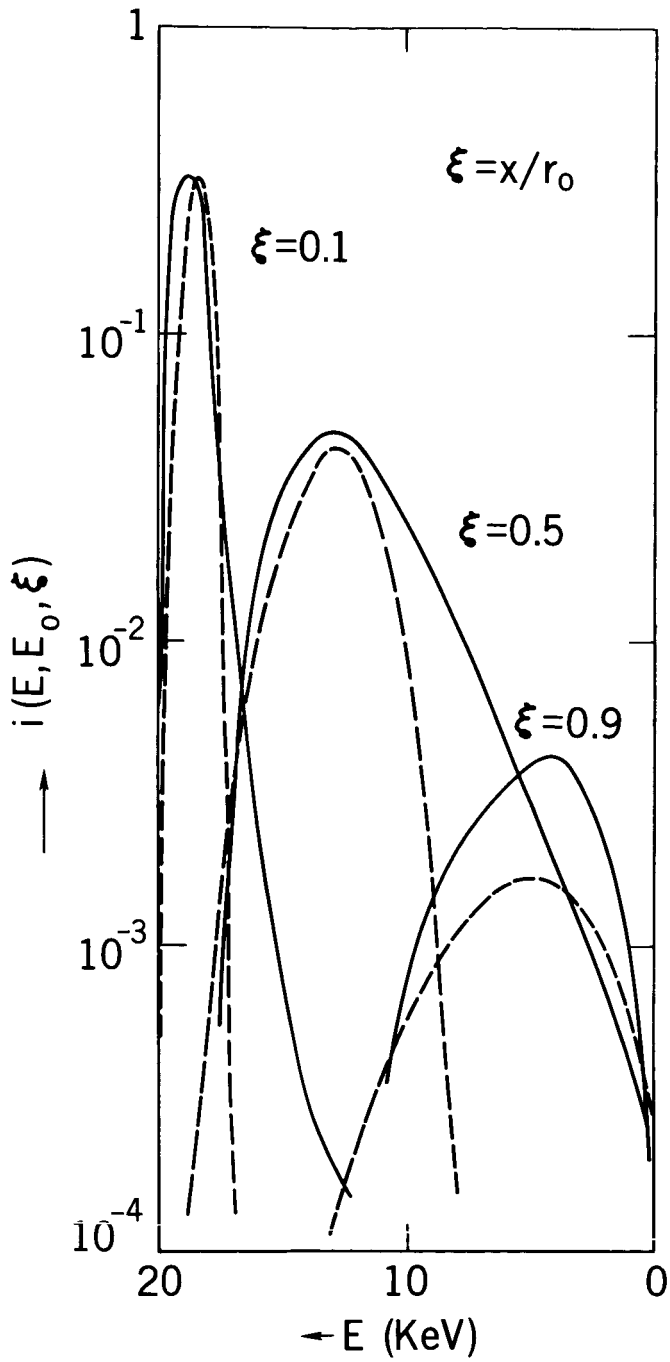

Figure 6–Comparison of $i(E, E_0, x)$ given by the formula (A-6) (dashed lines) and that of Monte Carlo calculation for the vertically incident monoenergetic electrons of E_0 = 20 kev (full lines).

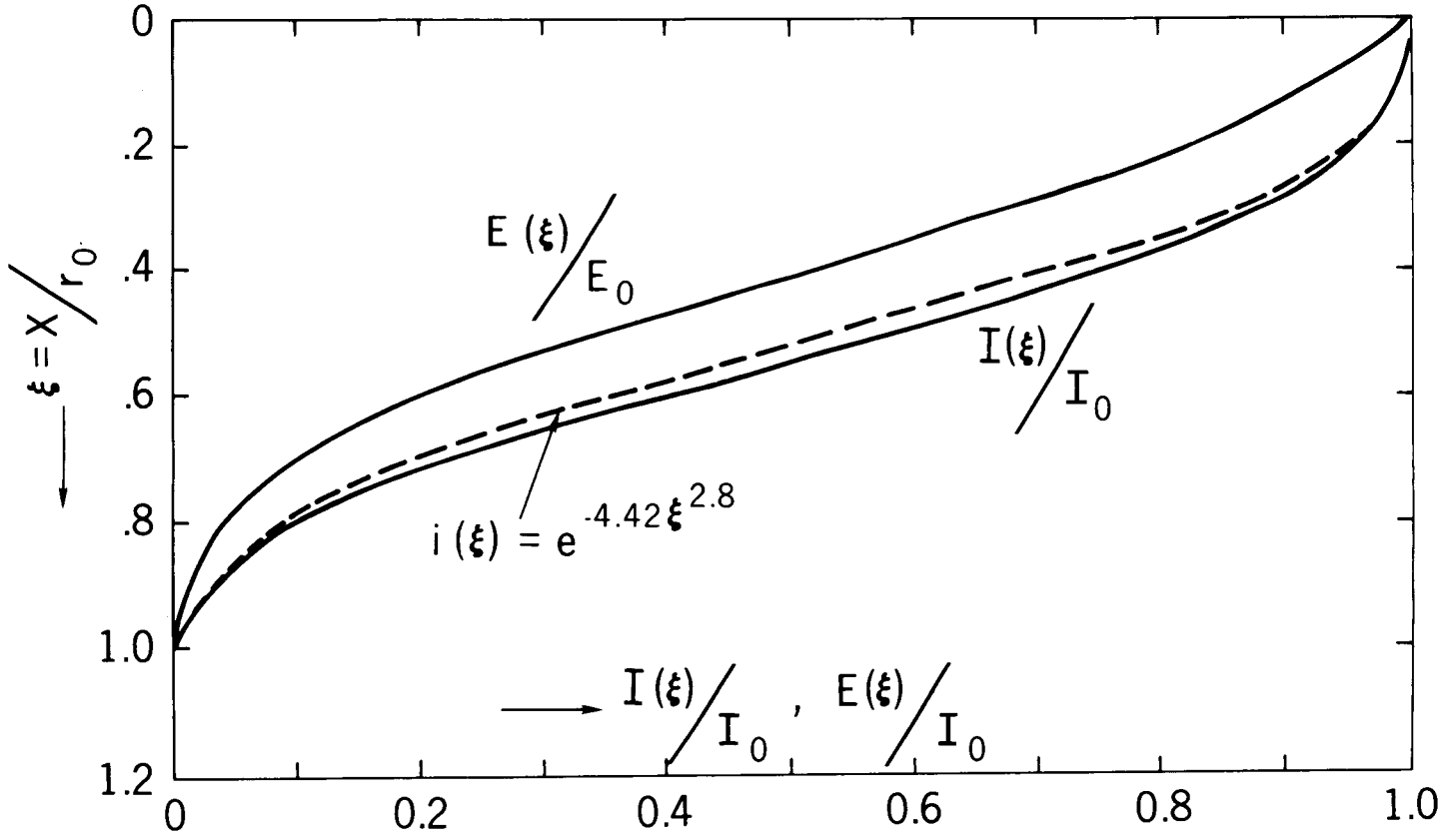

Figure 7–Variations of the total intensity of vertically incident monoenergetic electrons with the atmosphere depth,

$$I(E_0, \xi) = \int_0^{E_0} i(E, E_0, \xi)\, dE$$

where

$$\xi = X/r_0, \ (r_0 = 9.824 \cdot 10^{-4} \text{ g cm}^{-2} \text{ for } E_0 = 20 \text{ keV})$$

Full line and dashed lines stand for the results of Monte Carlo calculation and empirical expression, (A-1), respectively. Another full line indicate the Monte Carlo result of variation of total energy flux of vertically incident monoenergetic electrons.

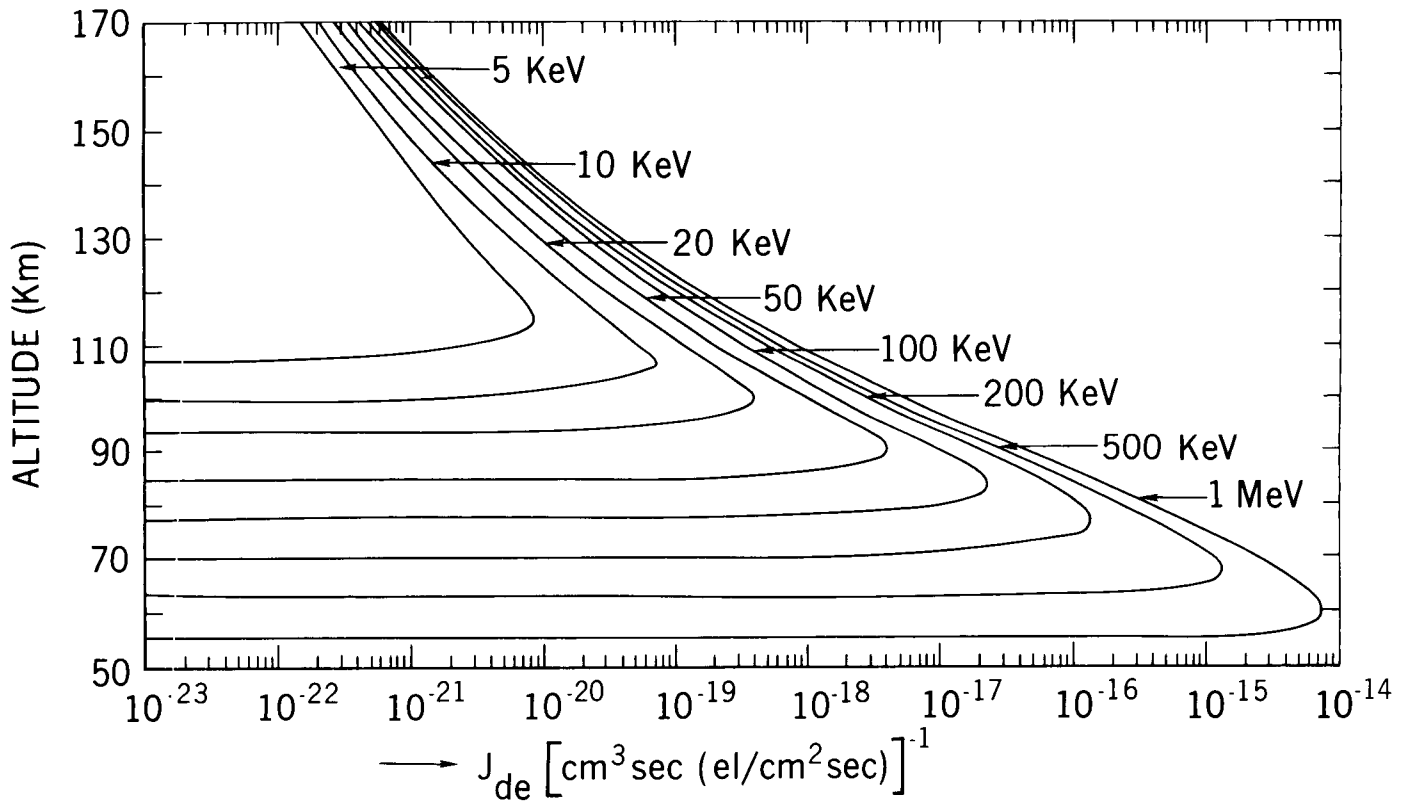

Figure 8–Rate of O_2-dissociation by monoenergetic auroral electrons (with energy E_0) as a function of altitude z (in km) for 5 kev $\leq E_0 \leq$ 1 Mev.

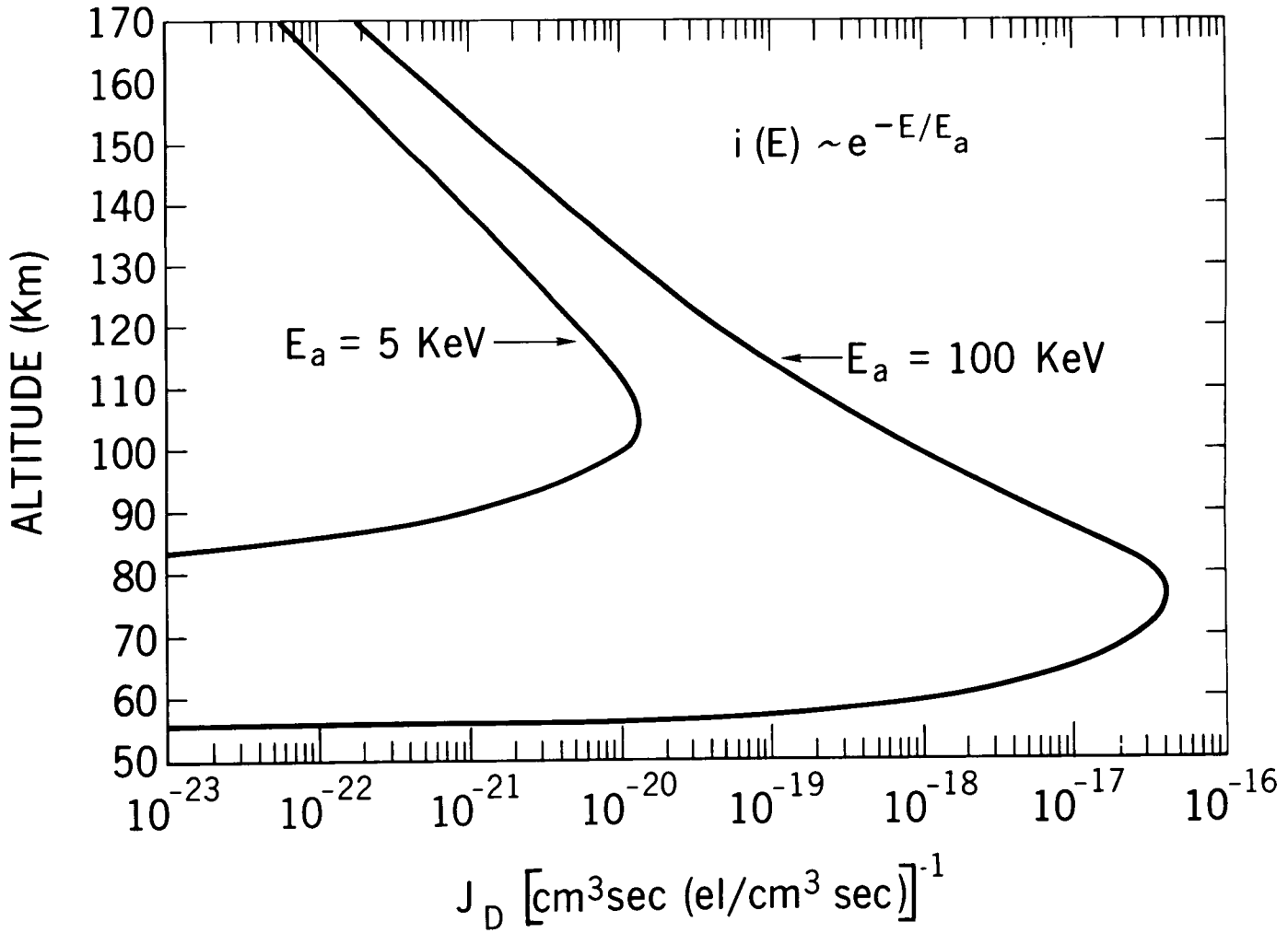

Figure 9–Rate of 0_2-dissociation by auroral electrons with energy e^{-E_0/E_a} vs. altitude z. Two curves correspond to E_a = 5 kev and E_a = 100 kev, respectively.

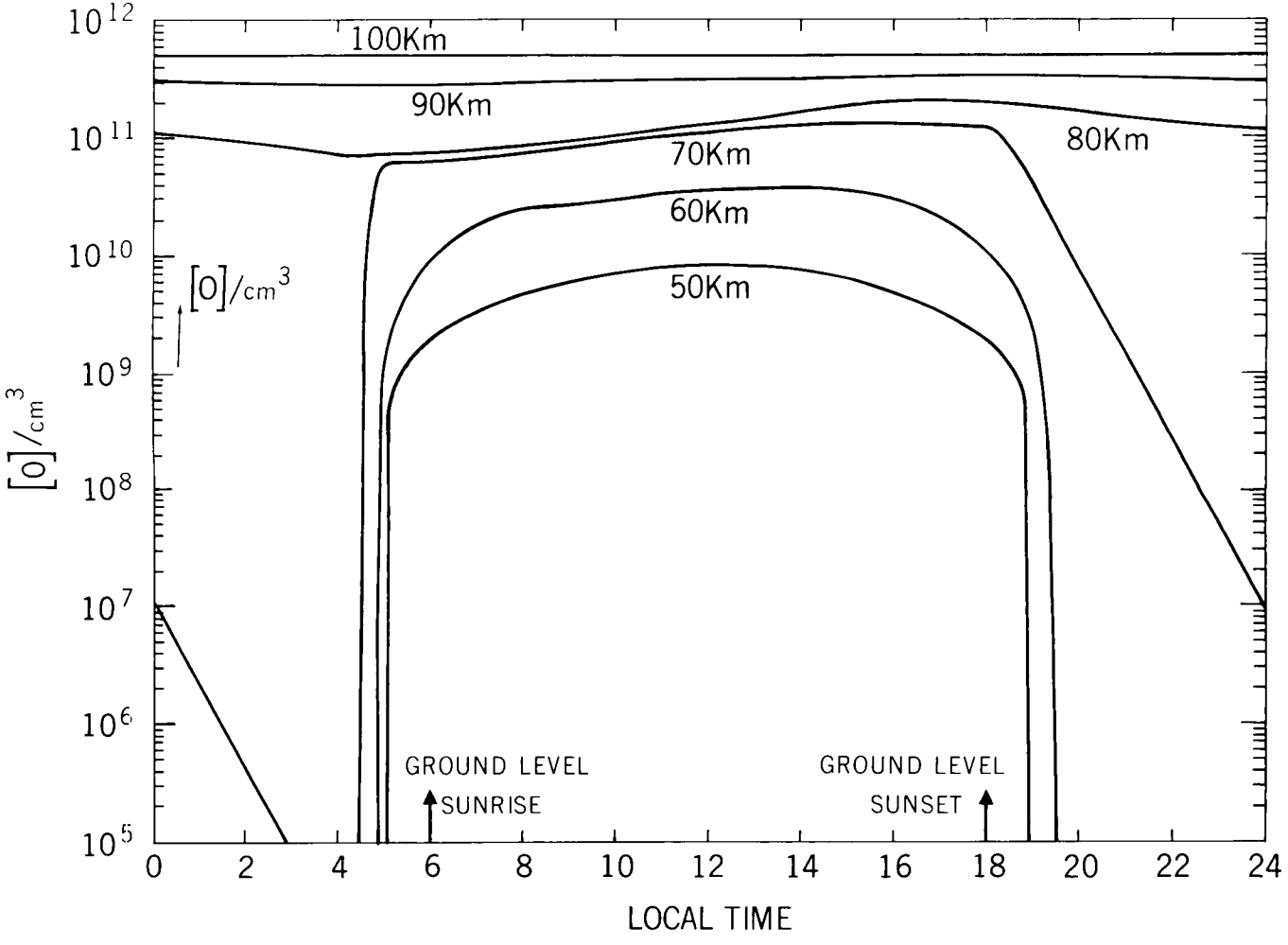

Figure 10–Diurnal variation of atomic oxygen (per cm^2) at each level from 50 km to 100 km intervals in equatorial atmosphere at the summer solstice.

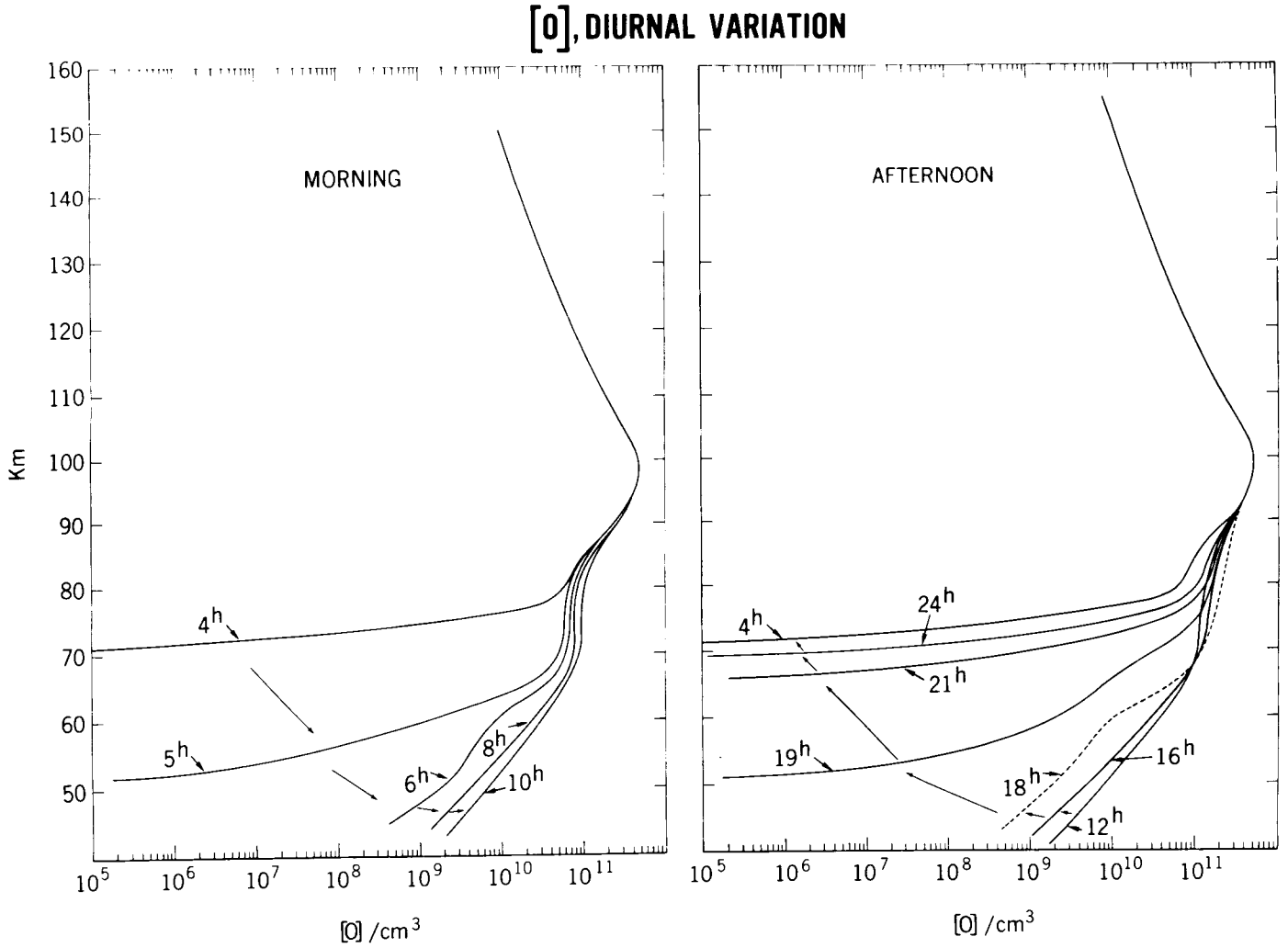

Figure 11–Diurnal variation of vertical distribution of atomic oxygen with time as a parameter, where the increasing phase after sunrise, and decreasing phase of variation in the afternoon are shown separately in (a) and (b), respectively.

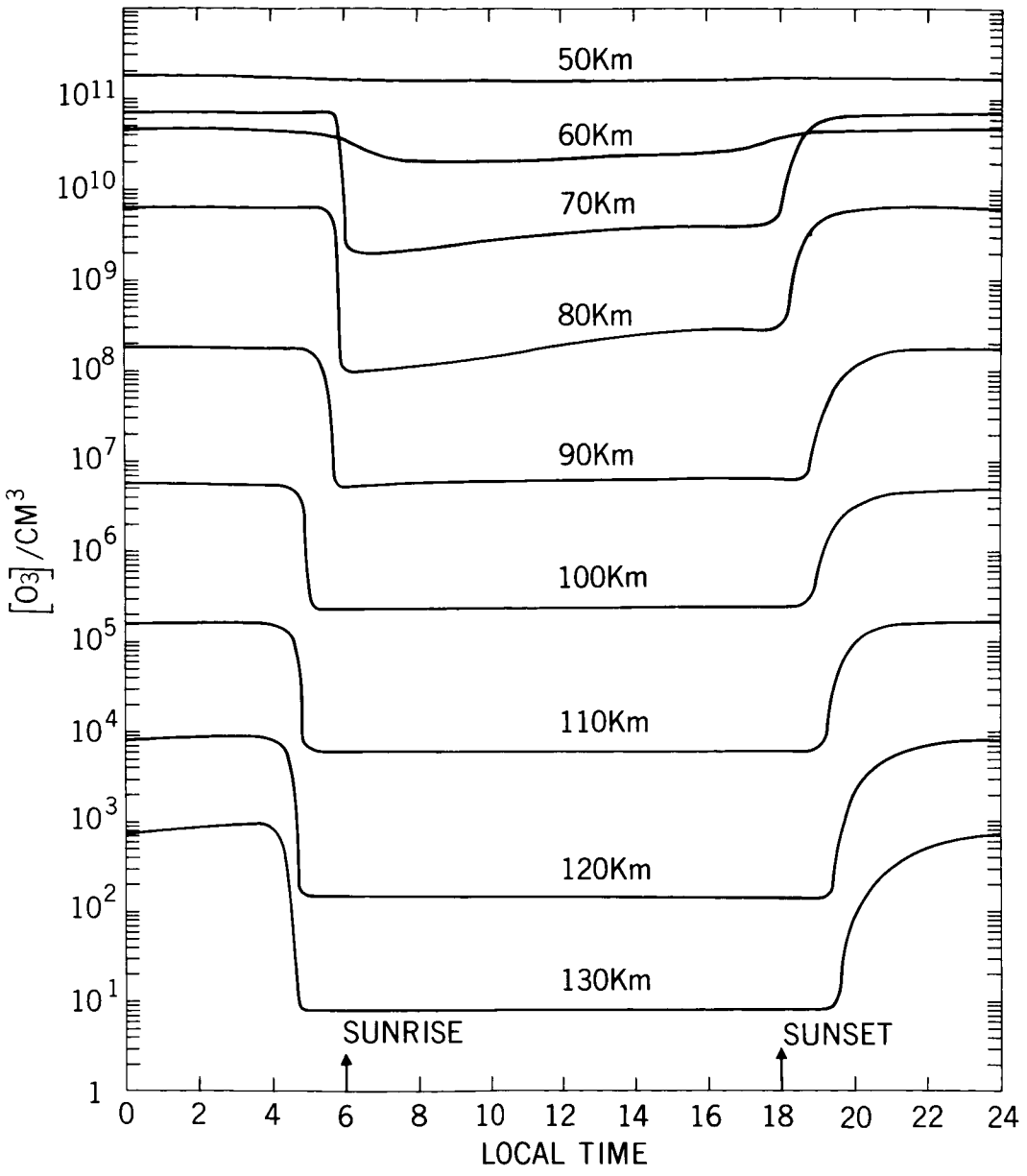

Figure 12–Diurnal variation of ozone at each level corresponding oxygen-atom variations shown in Fig. 10, in the equatorial atmosphere at summer solstice.

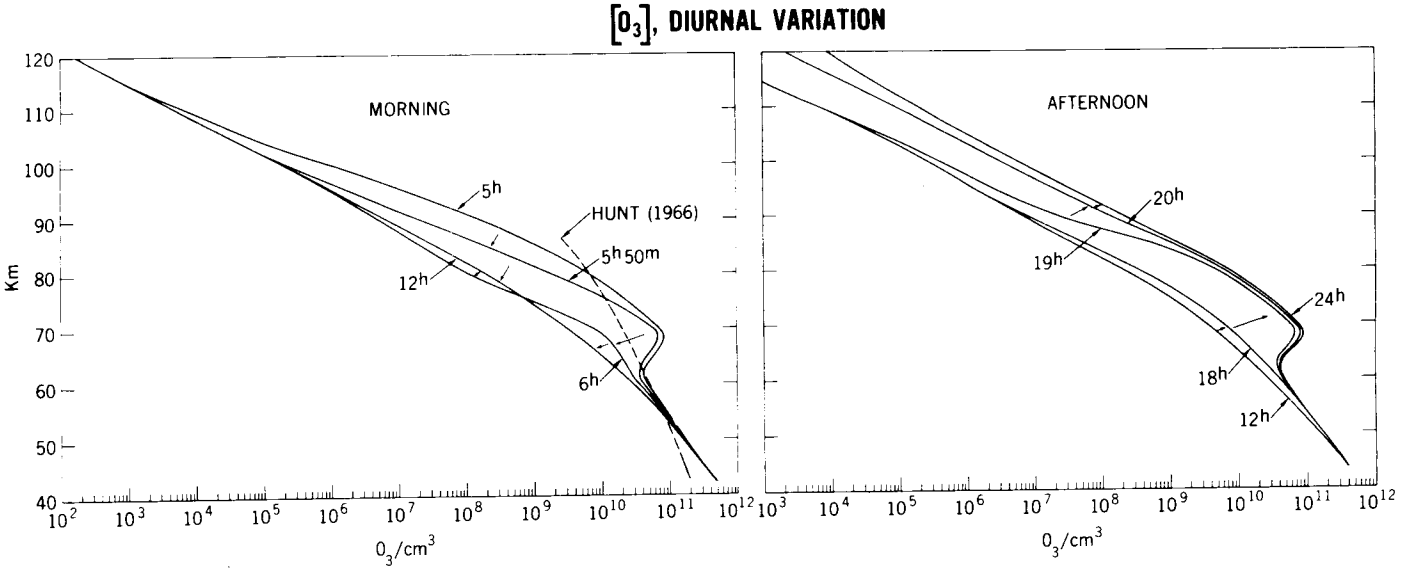

Figure 13–Vertical cross section of temporal variation of ozone shown in Fig. 12. To see the two phases of variation, the increasing – and decreasing phases are shown separately.

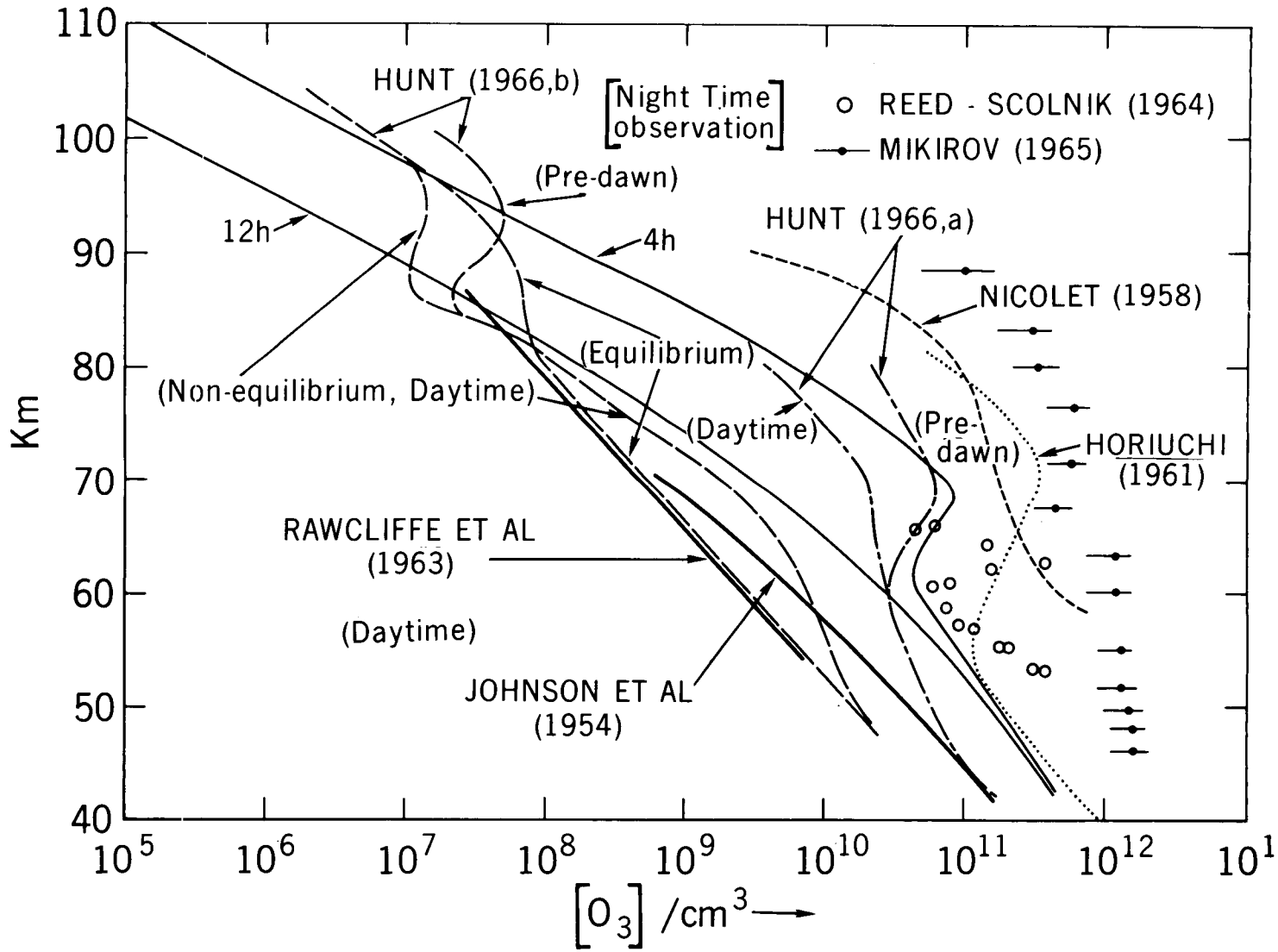

Figure 14–Comparison of observed values and theoretical results of ionospheric ozone distributions at the daytime equilibrium and nighttime enhancement. (i) Full lines, present calculations, (ii) Dash-dot lines, Hunt's pure oxygen atmosphere results (iii) Dashed-lines, Hunt's oxygen-hydrogen atmosphere results. (iv) Heavy lines, Rawcliffe et al. satellite observation and Johnson et al. rocket observation (v) Dotted lines, Nicolet's calculation for 10^4 sec after sunset and Horiuchi's calculation for 3.10^4 sec after sunset (vi) data points indicated by circles, Reed-Scolnik by UV-star light spectrum measurements (vii) data indicated by small dot with horizontal bar, Mikirov's data obtained by rocket observation of UV-moon light attenuation.

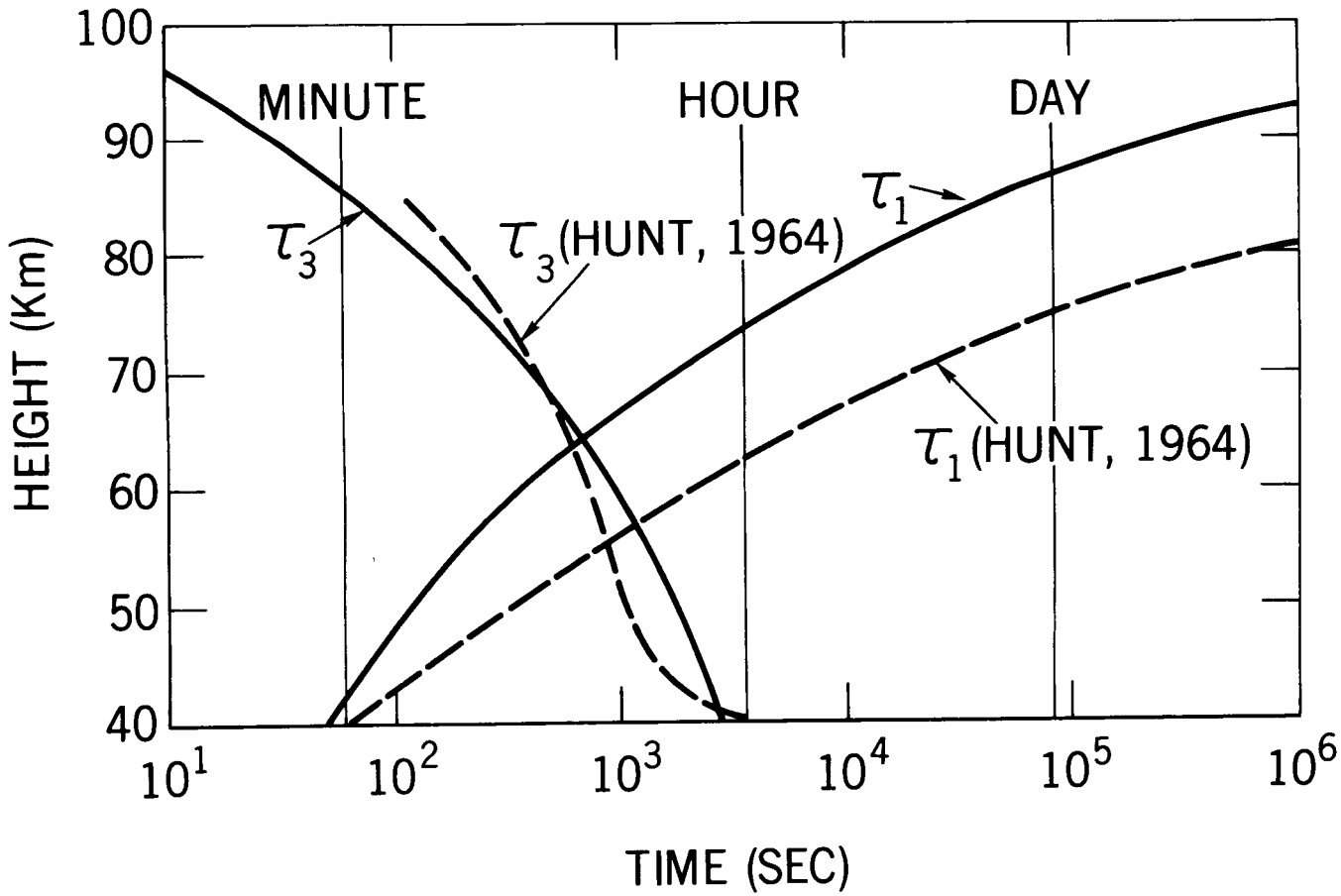

Figure 15–Time constants of atmospheric oxygen-atom, τ_3 (in sec), with comparison with Hunt's (1966) results (dashed line).

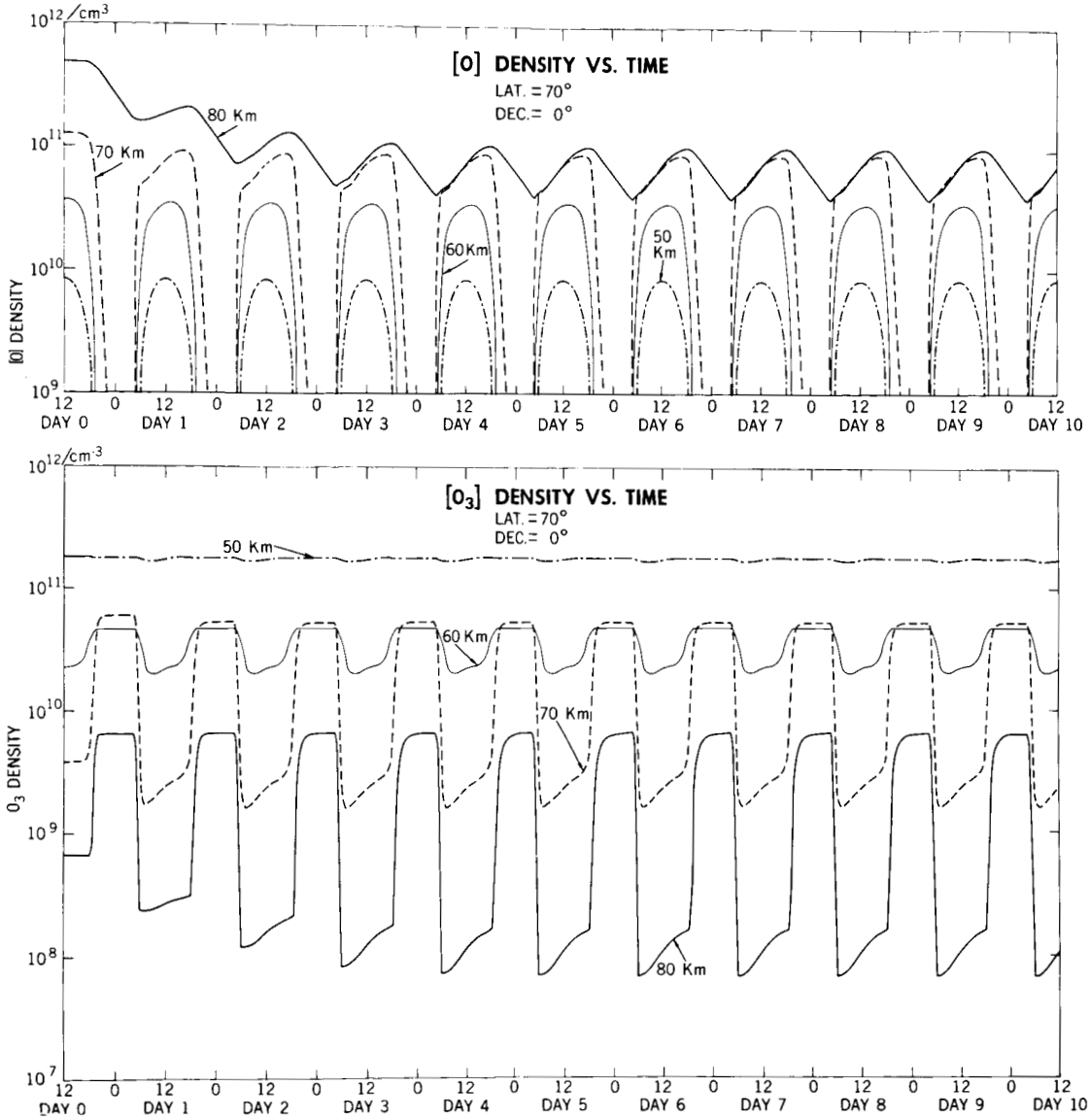

Figure 16(a)–Temporal variation of ozone and atomic oxygen in the polar hemisphere at the geographic latitude $\lambda = 70°$ and solar declination $\delta = 0$, equinox.

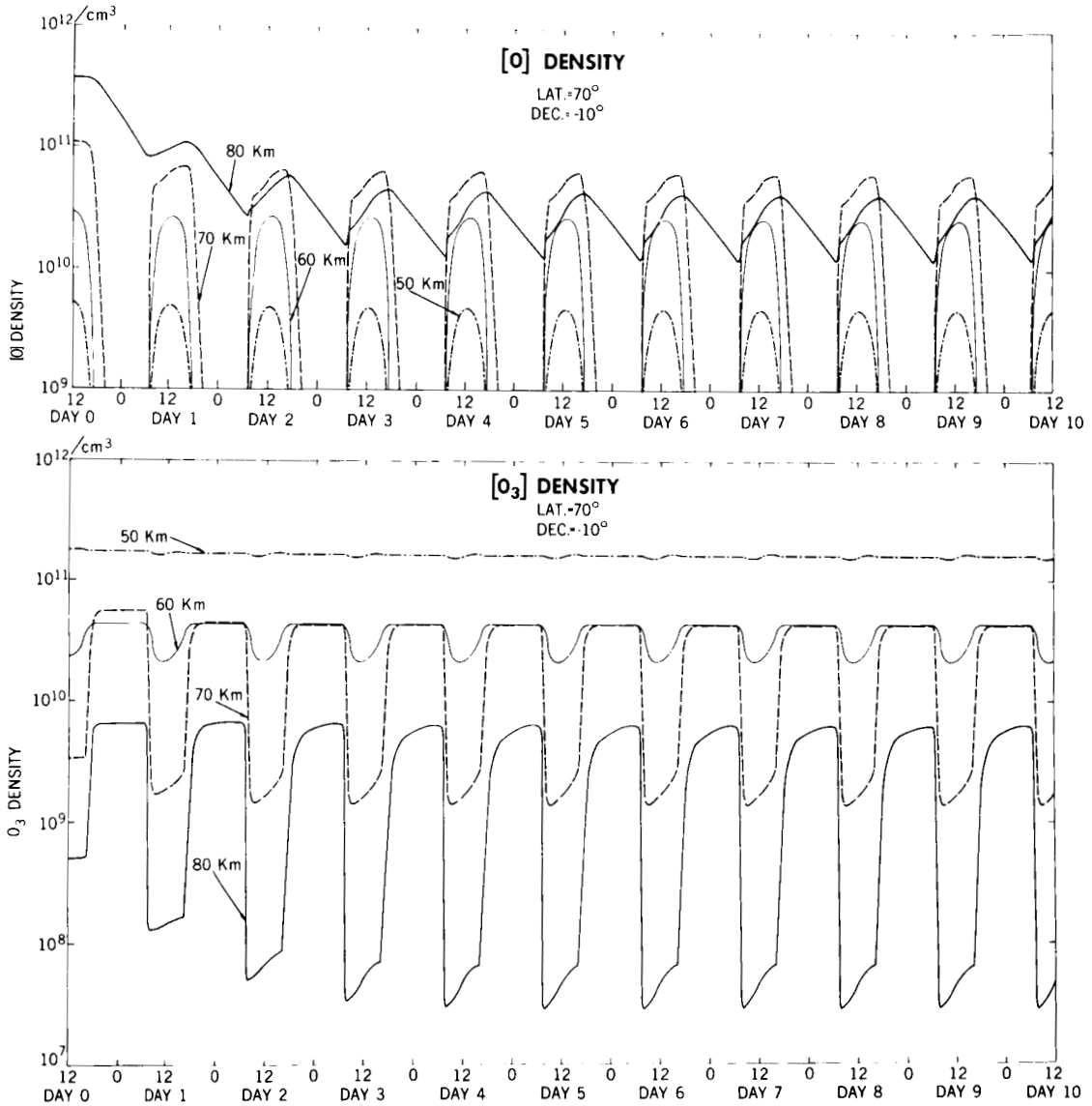

Figure 16(b)–Temporal variation of ozone and atomic oxygen in the polar hemisphere at the geographic latitude $\lambda = 70°$ and δ □ – 10°.

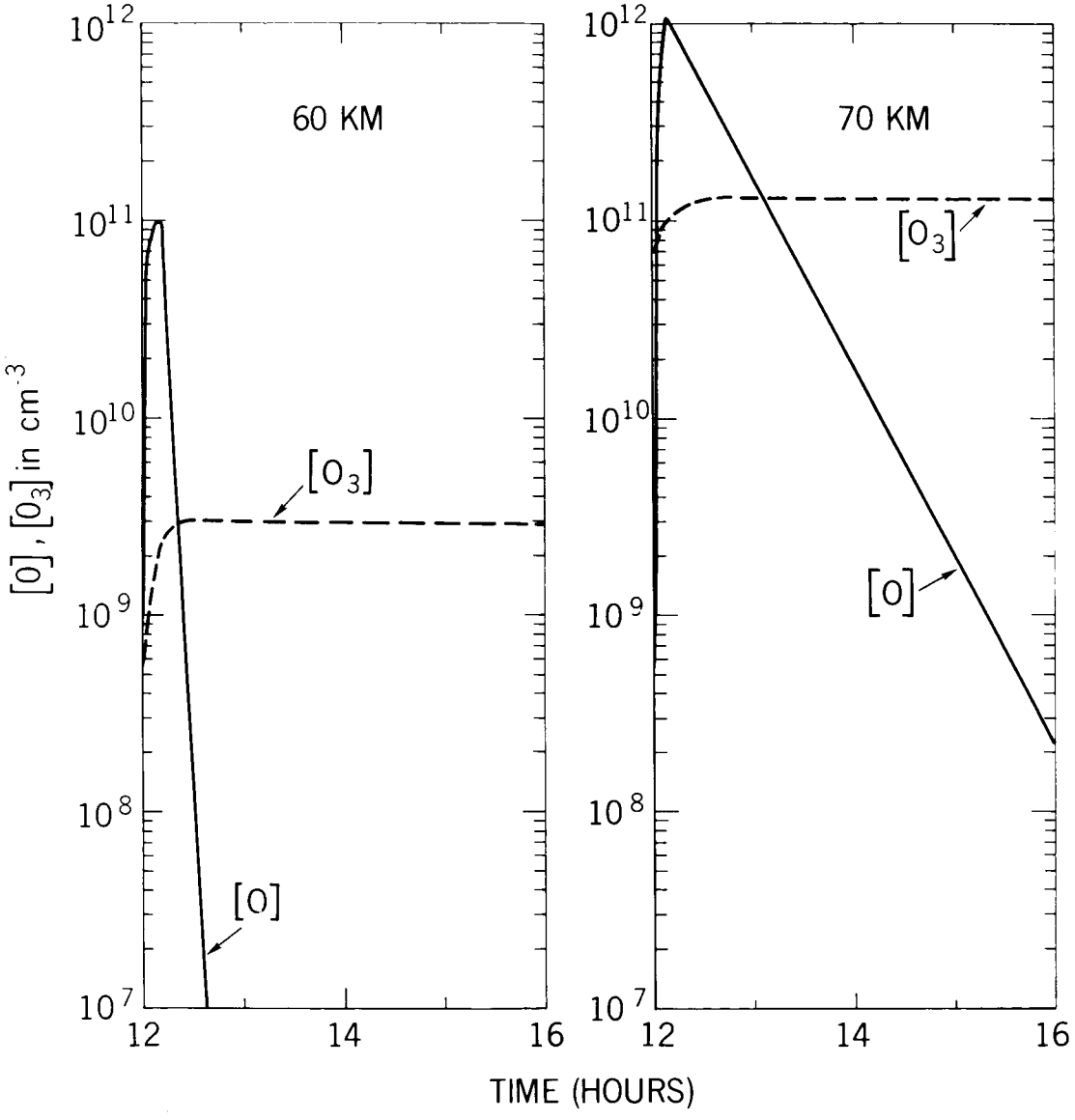

Figure 17(a)–Variation of 0- and 0_3 - concentration during and after the hard spectrum electron precipitation at 60 and 70 km, for $J_3 = J_2 \times 10^2$ and $i_0 = 10^{11}$ cm^{-3} sec^{-1}.

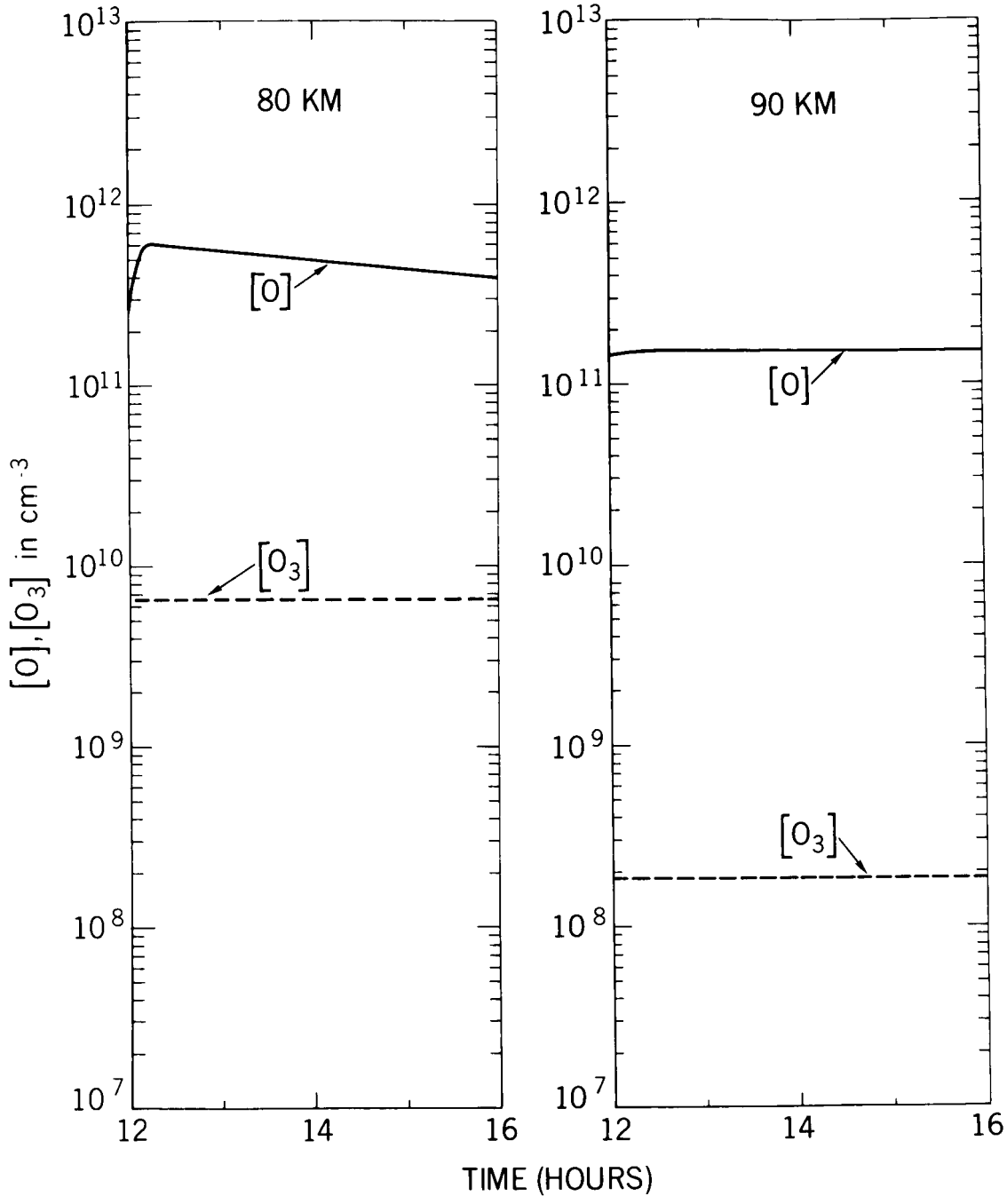

Figure 17(b)–Variation of 0- and 0_3 – concentration during and after the hard spectrum electron precipitation at 80 and 90 km, for $J_3 \sim J_2 \times 10^2$ and $i_0 = 10^{11}$ cm^{-3} sec^{-1}.

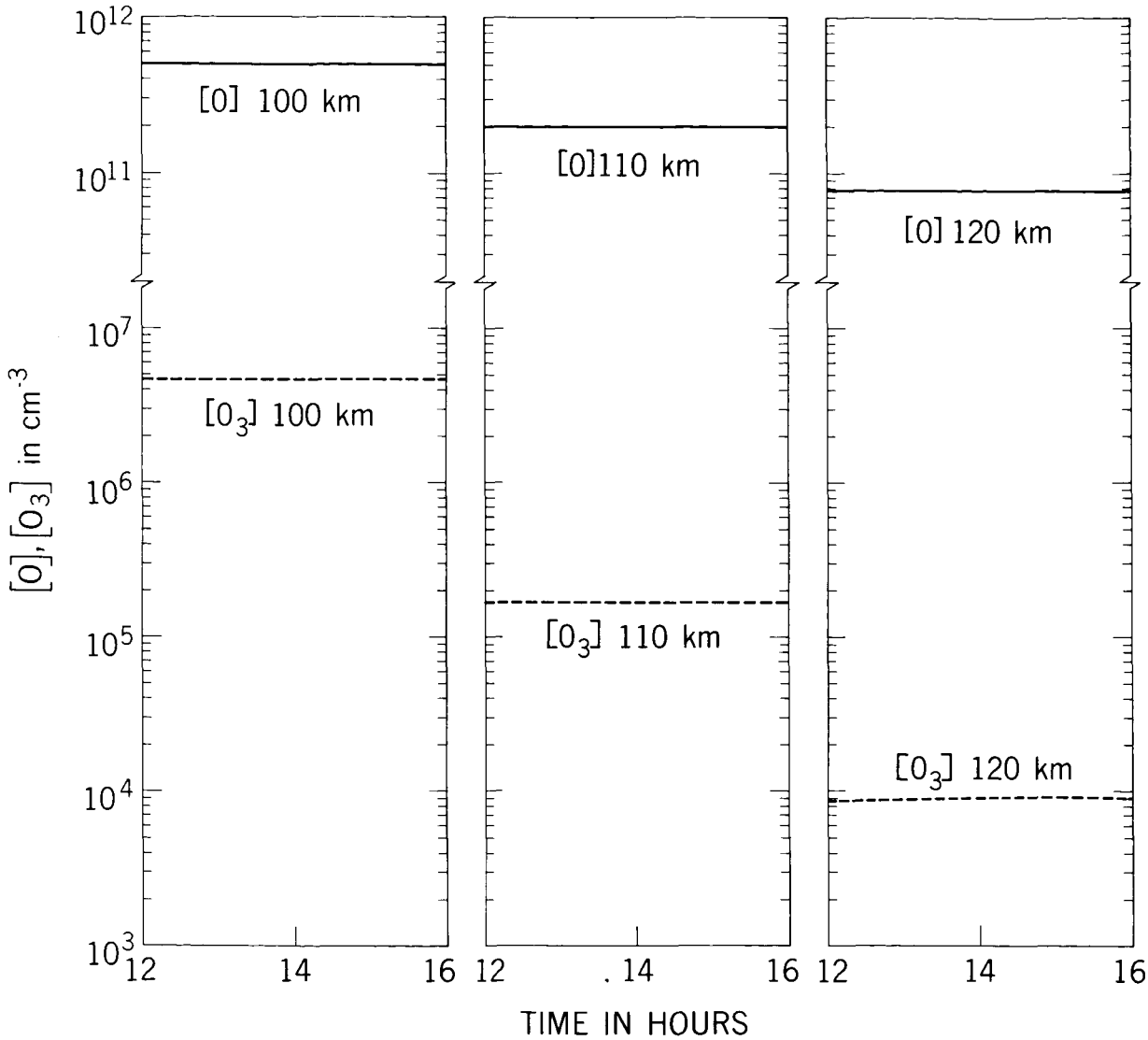

Figure 17(c)–Variation of O- and O_3 – concentration during and after the hard spectrum electron precipitation at 100, 110, and 120 km for $J_3 = J_2 \times 10^2$ and $i_0 = 10^{11}$ cm^{-3} sec^{-1}.

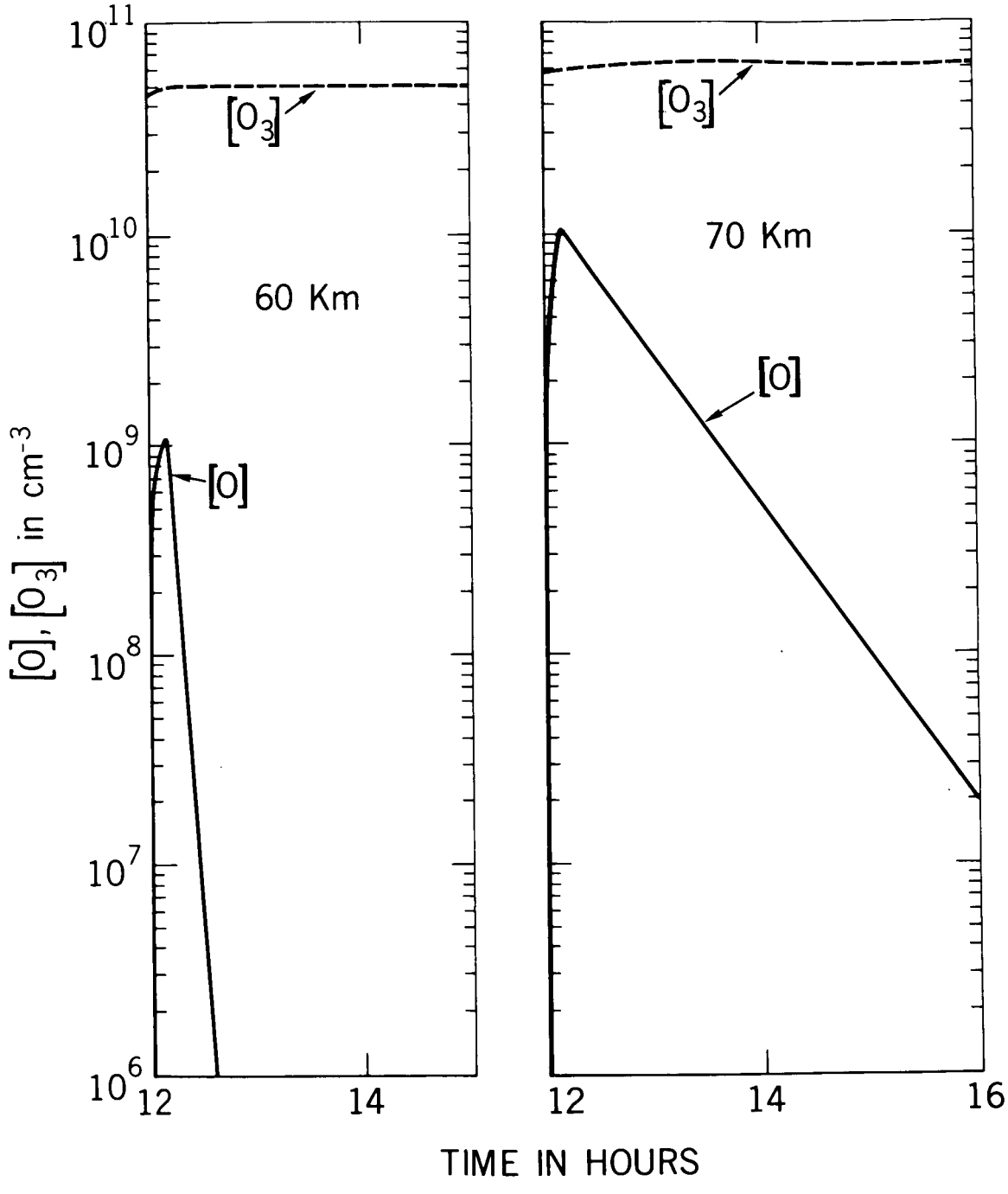

Figure 18(a)–The same as Figure 17 except $J_3 = J_2$.

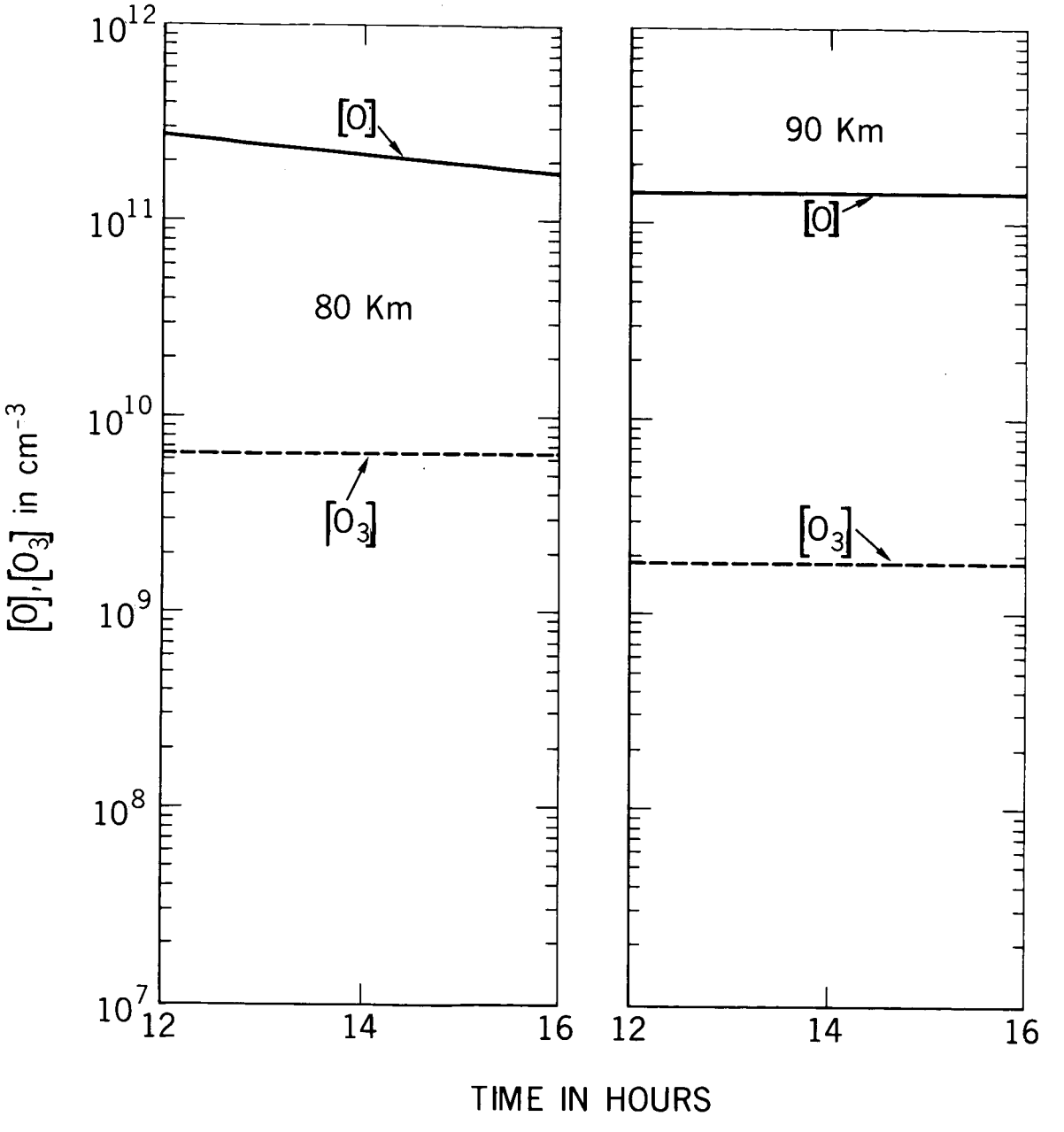

Figure 18(b)—The same as Figure 17 except $J_3 = J_2$.

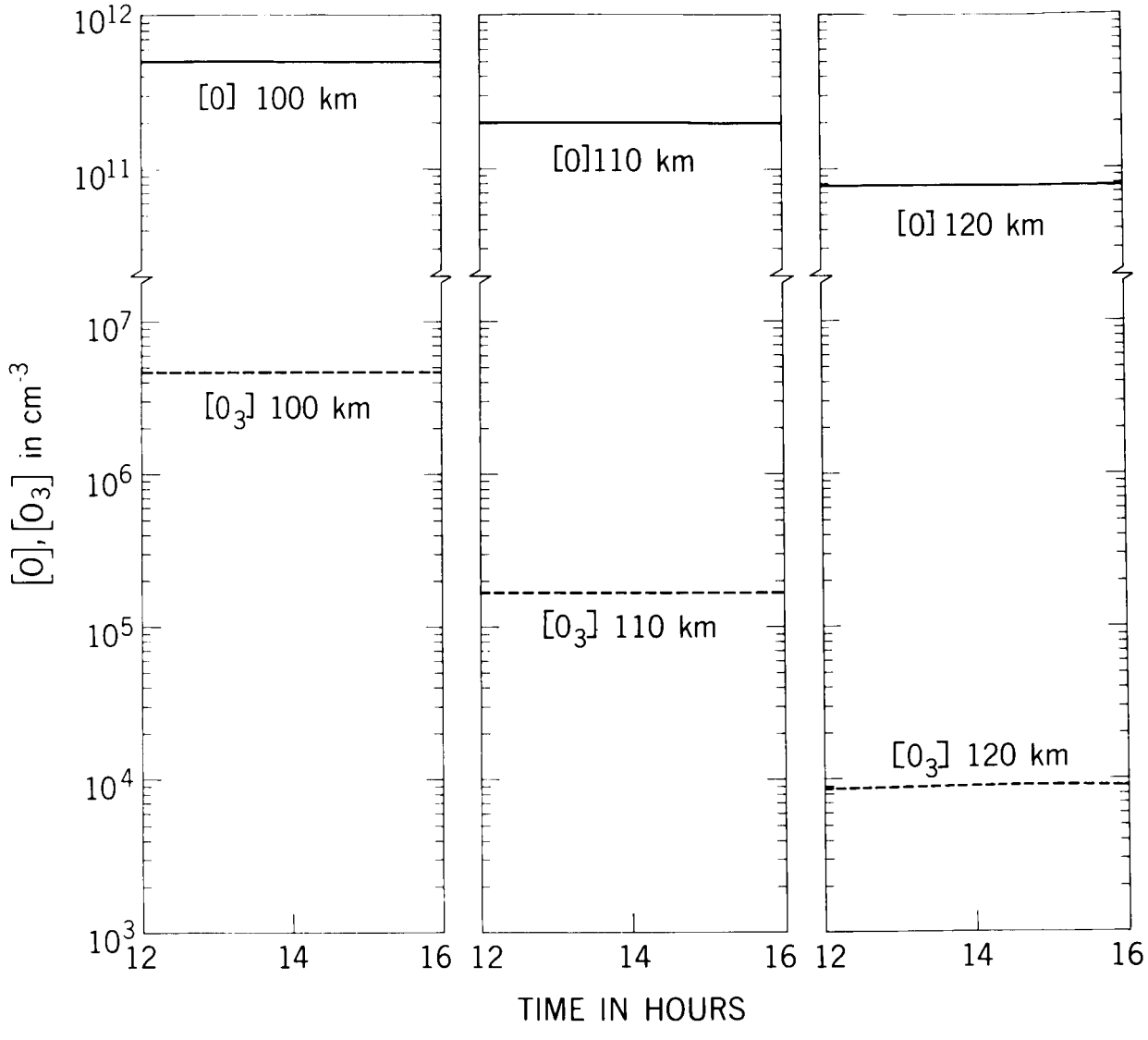

Figure 18(c)–The same as Figure 17 except $J_3 = J_2$.

VARIATIONS OF ATMOSPHERIC OXYGEN ATOMS CAUSED BY HARD SPECTRUM AURORA

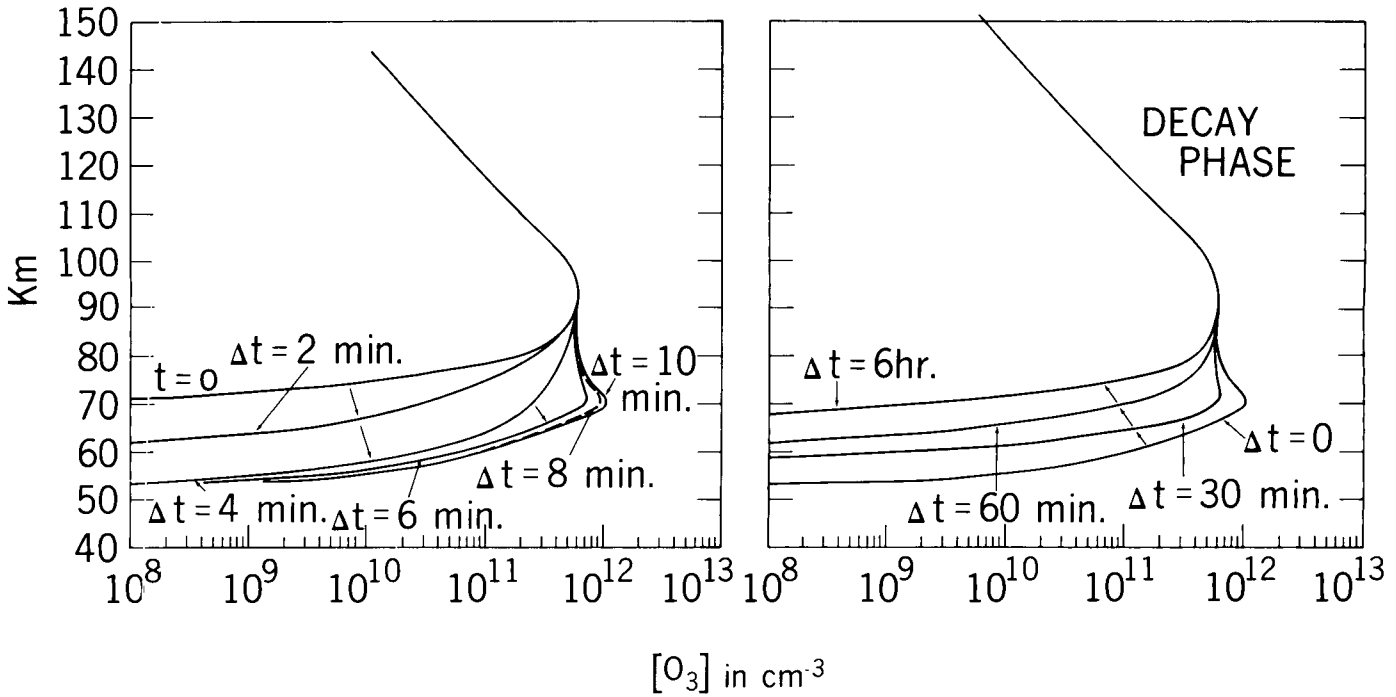

Figure 19–Variation of vertical distribution of atomic oxygen due to the hard spectrum electron precipitation (a) during electron precipitation (increasing phase) (b) after the ceased precipitation of $J_3 = J_3 \times 10^2$ and $i_0 = 10^{11}$ cm^{-2} sec^{-1}.

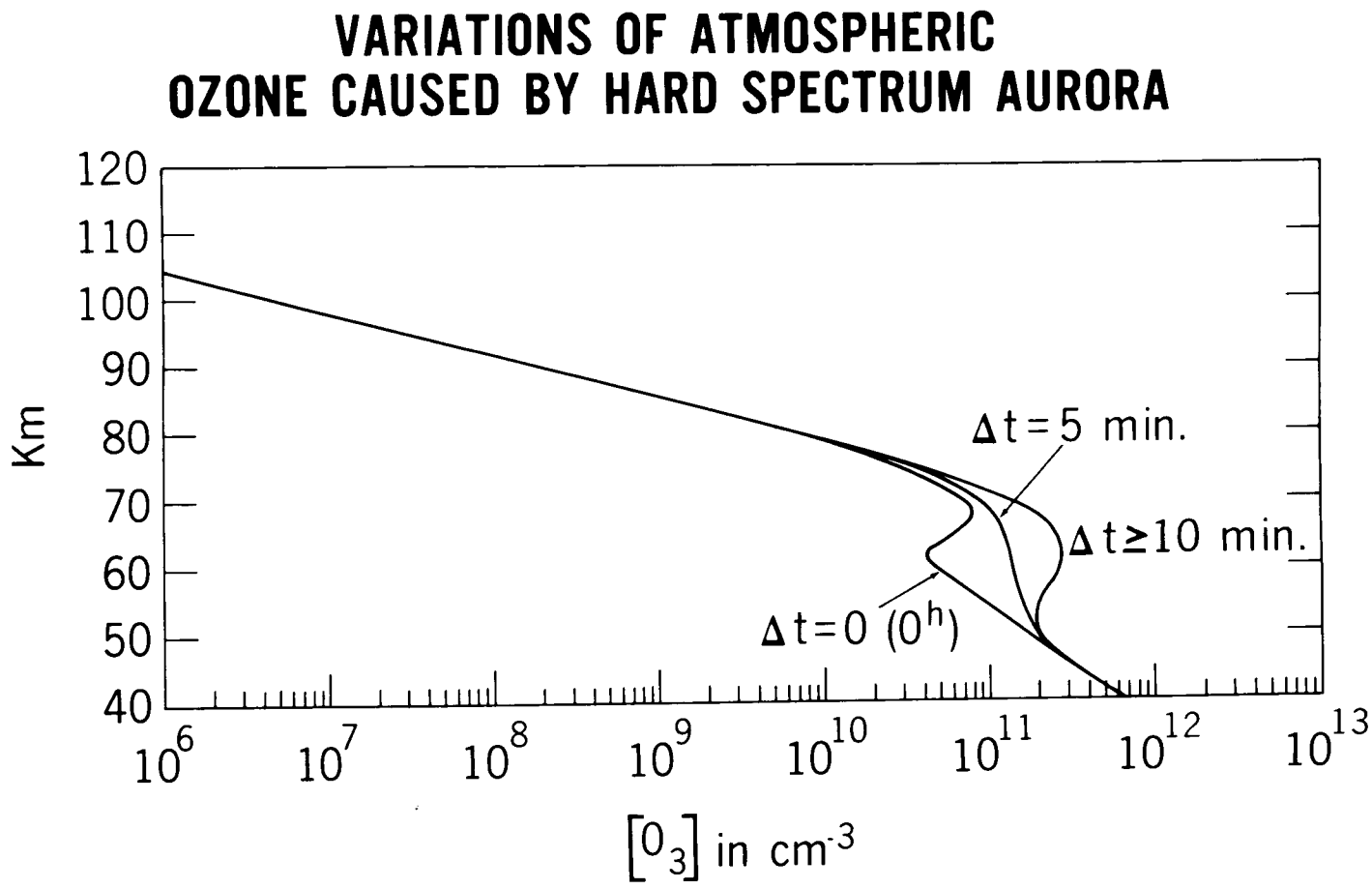

Figure 20–Variation of vertical distribution of ionosphere ozone during and after the hard spectrum electron precipitation for $J_3 = J_2 \times 10^2$ and $i = 10^{11}\,cm^{-2}\,sec^{-1}$.